Earth Surface Processes and Landforms

Tidal inlets in the Anthropocene: geomorphology and benthic habitats of the Chioggia inlet, Venice Lagoon (Italy)

Journal:	*Earth Surface Processes and Landforms*
Manuscript ID	ESP-18-0189
Wiley - Manuscript type:	Special Issue Paper
Date Submitted by the Author:	30-Apr-2018
Complete List of Authors:	Fogarin, Stefano; Universita Ca' Foscari, Department of Environmental Sciences, Informatics and Statistics; Istituto di Scienze Marine Consiglio Nazionale delle Ricerche, Madricardo, Fantina; Istituto di Scienze Marine Consiglio Nazionale delle Ricerche, ISMAR - Venezia Zaggia, Luca; Istituto di Scienze Marine Consiglio Nazionale delle Ricerche, ISMAR - Venezia Sigovini, Marco; Istituto di Scienze Marine Consiglio Nazionale delle Ricerche, ISMAR - Venezia Montereale-Gavazzi, Giacomo; Royal Belgian Institute of Natural Sciences, Natural sciences; Ghent University, Renard Centre of Marine Geology, Department of Geology and Soil Science Kruss, Aleksandra; Istituto di Scienze Marine Consiglio Nazionale delle Ricerche, ISMAR - Venezia Lorenzetti, Giuliano; Istituto di Scienze Marine Consiglio Nazionale delle Ricerche, ISMAR - Venezia Manfè, Giorgia; Istituto di Scienze Marine Consiglio Nazionale delle Ricerche, ISMAR - Venezia Petrizzo, Antonio; Istituto di Scienze Marine Consiglio Nazionale delle Ricerche, ISMAR - Venezia Molinaroli, Emanuela; Università Ca’ Foscari, Dipartimento di Scienze Ambientali Trincardi, Fabio; Istituto di Scienze Marine Consiglio Nazionale delle Ricerche, ISMAR - Venezia
Keywords:	Tidal inlet, MultiBeam EchoSounder, Benthic Habitat Mapping, Venice Lagoon
Note: The following files were submitted by the author for peer review, but cannot be converted to PDF. You must view these files (e.g. movies) online.	
Appendix1.xls	

Tidal inlets in the Anthropocene: geomorphology and benthic habitats of Chioggia inlet, Venice Lagoon

Fogarin*[1,2], S., Madricardo[2], F., Zaggia[2], L., Sigovini[2], M., Montereale-Gavazzi[3,4], G., Kruss[2], A., Lorenzetti[2], G., Manfé[2], G., Petrizzo[2], A.,Molinaroli[1], E., Trincardi[2], F.

[1] University of Ca' Foscari, Venice, Italy

[2]Institute of Marine Sciences, CNR, Venice, Italy

[3]Royal Belgian Institute of Natural Sciences, Brussels, Belgium

[4]Renard Centre of Marine Geology, Department of Geology and Soil Science, University of Ghent, Belgium

Within a multidisciplinary approach, we mapped with unprecedented detail the seafloor morphology, sediment distribution and benthic habitats of a tidal inlet which has been highly impacted by human activity. We identified an unusual habitat for lagoon environment connected to rip-rap used for jetties and hard structures and we estimated that the new pattern of flow around these hard structures caused the erosion of 430'000 m^3 of sediment in 8 years.

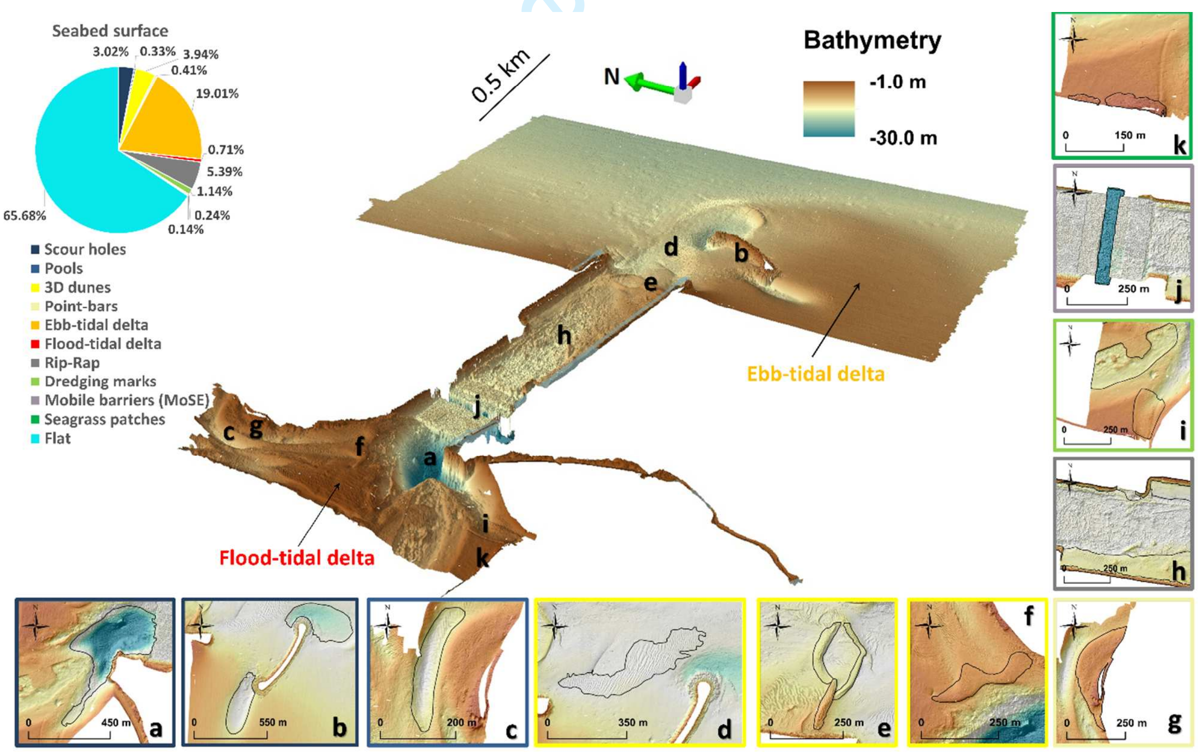

Tidal inlets in the Anthropocene: geomorphology and benthic habitats of the Chioggia inlet, Venice Lagoon (Italy)

Fogarin[1,2], S., Madricardo[2], F., Zaggia[2], L., Sigovini[2], M., Montereale-Gavazzi[3,4], G., Kruss[2], A., Lorenzetti[2], G., Manfé[2], G., Petrizzo[2], A., Molinaroli[1], E., Trincardi[2], F.

[1] Department of Environmental Sciences, Informatics and Statistics (DAIS), Università Ca' Foscari Venezia, Campus Scientifico, Via Torino 155, Mestre, VE, Italy

[2] Istituto di Scienze Marine-Consiglio Nazionale delle Ricerche, Arsenale - Tesa 104, Castello 2737/F, 30122 Venezia, Italy

[3] Royal Belgian Institute of Natural Sciences, Operational Directorate Natural Environment

Gulledelle 100, 1200 Brussels, Belgium

[4] Renard Centre of Marine Geology, Department of Geology and Soil Science, University of Ghent

Abstract

Within a multidisciplinary approach, we mapped with unprecedented detail the seafloor morphology, sediment distribution and benthic habitats of a tidal inlet which has been highly impacted by human activity. Thanks to very high resolution multibeam data, we describe the ebb and flood tidal deltas, a tidal point bar, dune fields, large dunes, pools and scour holes.

The inlet seafloor substrate composition was investigated by comparing automatically classified multibeam backscatter data, with data from sediment samples and underwater sea-floor images. We identified four textural classes with 75% overall thematic accuracy. In this way, we recognized the sediment distribution of each morphological feature. In particular, we could distinguish the sediments over crests and troughs of small-dune fields with wavelengths and heights of less than 4 m and 0.2 m, respectively.

Adopting the latest benthic habitat mapping procedures, we identified seven different benthic habitats inside the tidal inlet in relation to hydrodynamics sediment transport pathways and marine life. The dominant classes were *Sand with bioclasts* (46%) and *Bare sand* (32%). The rip-rap revetment used for the inlet jetties and for the hard structures, built in the inlet channels to protect Venice from flooding, created a new habitat that accounted for 5.51 % of the study area surface. We estimated that the new pattern of flow around these hard structures also caused the erosion of 430’000 m^3 of sediment in 8 years. This study shows that by combining the geomorphological and ecological perspectives it is possible to improve the monitoring and management of tidal inlets and coastal infrastructures.

Keywords: Tidal inlet, MultiBeam Echosounder, benthic habitat mapping, Venice Lagoon

Introduction

Coastal lagoons are transitional environments connecting land and sea. They occupy about 13% of the world's coastlines (Bird, 1994; Kjerfve, 1994). These regions, together with coastal ecosystems, are an important part of ecological heritage (Costanza et al., 1997; Luisetti et al., 2014). Historically, coastal lagoons, estuaries and deltas have played an important role in human geography: these sites usually host intensive agriculture and industry, high population and hard infrastructures (Gönenç and Wolflin, 2005). Coastal lagoons communicate with the sea by one or more littoral openings (inlets), which allow the exchange of water (Kjerfve, 1994). The inlet formation during storms is an important control on the dynamics and evolution of barrier islands separating the lagoon from the sea (Davidson-Arnott, 2010). The sustainable management of transitional ecosystems cannot ignore the key-role of the inlets, considering that they: (i) control hydrodynamics and the chemical-physical properties of the lagoon, (ii) are responsible for the sediment transport from the lagoon to the open sea and vice versa, (iii) affect the morpho-dynamics of the adjacent coast, (iv) are often subject to intense maritime traffic, (v) allow the migration of different species at different life stages (Reddy et al., 2015). However, the lagoon inlets are quite fragile and change constantly (Duck and Silva, 2012): tidal conditions combined with geological, hydrological, ecological and climatic factors may alter the evolution of these systems (Wanless, 1981). Human interventions as well often play a major role inducing rapid morphological changes and a different equilibrium state (Williams, 2013). This anthropogenic forcing can radically unbalance the dynamics that the inlets would normally follow in natural conditions (Oost et al., 2012).

This is the case of the three inlets of the Venice Lagoon (Italy), the largest lagoon of the Mediterranean, surrounding the historical city of Venice. This lagoon has undergone strong changes in the Anthropocene era and can be considered as a "human-oriented ecosystem" (Cima and Ballarin, 2013). The term Anthropocene have been used to designate the rock unit and time interval where the impact of collective human action on the Earth system is clearly recognizable. Humans are altering the planet, including long-term global geologic processes, at an increasing rate. Any formal recognition of an Anthropocene epoch in the geological time scale hinges on whether humans have changed the Earth system sufficiently to produce a stratigraphic signature in sediments. There is great debate about the term Anthropocene (Hamilton, 2016; Finney and Edwards, 2016). In our study area the shift from the Holocene to the modified Holocene and, later, to the Anthropocene social-ecological system states (as defined in Renaud et al., 2013) could be set at the time of Serenissima Repubblica of Venice (starting from the end of 7th century), when the urbanization and regulation of the lagoon environment radically modified its natural evolution. In this framework, uninterrupted work was undertaken to avoid the filling up of the lagoon by deviating the major rivers that were flowing into it.

The natural inlets were radically reshaped by the construction of long jetties between 1808 and 1933 (Fontolan et al., 2007, Balletti et al. 2016). They were dredged and deepened from 5 m to 15 m with a consequent increase in tidal flow and erosive processes in the whole lagoon (Gatto and Carbognin, 1981, Tambroni and Seminara, 2006). The recent construction of a system of mobile barriers at the lagoon inlets in the past 15 years (the MoSE Project, Ministero dell'Ambiente - Magistrato alle Acque, 1997) resulted in more major engineering interventions at the inlets . These barriers should defend the city of Venice and the other islands in the lagoon from flood events (see Trincardi et al. 2016 for the background). The mobile barriers represent a paradigmatic example of response to flooding also in view of global mean sea level rise (Temmerman et al., 2013; Perkins, 2015).

Several studies concerning the Venice Lagoon inlet hydrodynamics and sediment transport exist (Fontolan et al., 2007; Amos et al., 2010; Defendi et al., 2010; Villatoro et al., 2010). Nevertheless, the submarine geomorphology and the sediment distribution are less well documented, especially in relationto human driven alterations. In this study, a state-of-the-art MultiBeam EchoSounder (MBES) was operated in shallow water (average depth less than 15 m) to survey the seafloor of the Chioggia inlet (Fig. 1). Through the collection and analysis of MBES data (namely depth and backscatter intensity), sediment samples and seafloor images, we described in detail the main morphological and sedimentological properties and main habitat classes of the study area seafloor. The evolution of tidal channel and their morphological properties were studied from different points of view with modeling studies and satellite data analysis, however, only recently the technological development of MBES has allowed for to map their seafloor morphological features in high resolution (Fraccascia et al., 2016).

Whereas the study of land use change in the Anthropocene start to be well established (Tarolli et al., 2016; Brown at al., 2017), much less is known about the human footprint on the seafloor. Indeed, less than 15% of the world's seafloor has been mapped so far (Meyer et al., 2018).

In this study we not only provide a very high resolution mapping of tidal inlets seafloor morphologies and habitats, but we also quantitatively assessthe physical changes induced by human activities and their impact on the tidal inlet habitats.

Geographical setting

The Lagoon of Venice is the largest in the Mediterranean Sea, with a surface area of 550 km^2 (Fig.1). The lagoon has a mean depth of about 1.2 m, with only 5% of its area deeper than 5 m (Molinaroli et al., 2009). The deepest point of the lagoon reaches almost 50 m and the main navigation channels easily reach depths of 20 m. The lagoon has been subject to anthropogenic modifications since historical times, dating as far back as 900 BC (Molinaroli et al., 2007). Without human intervention, the lagoon would have gradually silted up by the river sediment input. Therefore, starting from the 12th century the main tributary rivers were diverted directly into the sea (Cavazzoni, 1995, D'Alpaos, 2010; Madricardo and Donnici, 2014). Whereas during the times of the Serenissima (697-1797) the silting process dominated, a strong erosive process took place in the last century. Particularly, between 1970 and 2000, following the dredging of a large navigation channel from the Malamocco inlet to the industrial harbor, the lagoon morphology changed dramatically due to the erosion of salt marshes, overall deepening and tidal channel disappearance (Sarretta et al., 2010, Madricardo and Donnici, 2014). In fact, the lagoon, particularly in its central area, is gradually assuming the characteristics of a marine environment, a closed appendix of the Adriatic Sea (Carniello et al. 2009; Molinaroli et al. 2009; Sarretta et al., 2010). At least, a quarter of the lagoon habitats have been lost with a consequent change in the functionality of the systems (Favero, 1991; Elliot and Cutts, 2004).

The recent construction of the MoSE structures at the inlets could substantially affect the lagoon environment by reducing the tidal exchange through the inlets and increasing the ebb-dominance over tidal flats (Tambroni and Seminara, 2006; Ghezzo et al., 2010, Ferrarin et al. 2015).

The Chioggia Inlet

The Chioggia inlet (45°13'54 "N, 12°18'3"E WGS84, geographic coordinates) is the southernmost inlet of the Venice Lagoon and has a maximum water flow range of 5000-6000 m^3/s. The mean water discharge through the inlets varies with tide and current speed reaches a peak value of 0.5 m/s during syzygy (Gaèiæ et al., 2004). However, in extreme weather marine conditions the speed increases up to 2 m/s.

This inlet has undergone numerous human interventions during history. The most evident changes have started in 1912 with the construction of jetties, that were modified again in 1950. The recent works for the construction of MoSE reduced the inlet cross-section from 500 to 350 m and the seafloor depth changed significantly due to dredging (Villatoro et al., 2010).

The MoSE project in fact required: (I) the construction of a 500 m long breakwater on the seaside, southeast of the inlet, (II) the reinforcement of the jetties, (III) the creation of a refuge harbour with a double navigation lock, (IV) the excavation of a 24 m deep and 50 m wide recess for hosting the mobile gates and their concrete housing structures, (V) the stabilization of the seabed near the recess with the deposition of boulders and artefacts in concrete and (VI) the dredging and deepening of the channels close to the inlet.

3. Materials and methods

3.1. High resolution MBES Data

The acoustic data in Chioggia Inlet (about 10 km^2) were collected in October and November 2013 (about 4 weeks of work) by the Institute of Marine Science of National Research Council (ISMAR - CNR) using a Kongsberg EM2040 Dual-

169 Compact MBES pole-mounted on the CNR research vessel Litus, a 10 m long boat with only 1.5 m draft. The MBES has 800 beams (400 per swath) and during the survey, the frequency was set to 360 kHz. A Seapath 300 system with the supply of a Fugro HP differential Global Positioning System (DGPS) automatically registered the ship positioning (0.2 m accuracy). For the correction of pitch, roll, heave and yaw movements the Kongsberg motion sensor MRU 5 and a Dual Antenna GPS integrated in the Seapath was used. The sound velocity was continuously measured by a Valeport mini SVS sensor attached close to the two transducers.

178 CARIS HIPS and SIPS software (v.7 and 9.1) was used for processing multibeam data considering sound velocity, tide corrections and manual quality control tools. The bathymetry was created with a raster resolution of 0.5 m using the Swath Angles Weighting option with a Max Footprint size of 9 × 9. The data are referred to the local datum ‘Punta Salute 1897’, 23.56 cm lower than the national vertical level datum (IGM1942).

185 The backscatter was created combining the georeferenced backscatter rasters (GeoBaR) of each survey line on the software Fledermaus (v7.0) with a resolution of 0.5 m. GeoBars were produced after applying the Angle Varying Angle (AVG) correction to the raw data to remove the angular artifacts of sediment.

189 The bathymetric and backscatter data are then exported as a 32-bit raster files and imported in ArcGis (v10.2) for further analysis (ESRI, 2016).

191 3.1.1 Seafloor features

From the digital elevation model (DEM) obtained from the MBES bathymetric data, we computed in ArcGis the main terrain attributes: slope, broad Benthic Position Index (BPI) and Ruggedness (Lecours et al. 2017a; Lecours at al., 2017b). The BPI and ruggedness were calculated with BTM (Wright et al., 2005) with BPI inner and outer radius of 750 and 50 respectively and ruggedness radius of 11. The results are collected in appendix B.

These layers provide an understanding of the morphological complexity as well as representing the seafloor's variability as governed by hydrodynamic conditions and sediment accretion or erosion (Ierodiaconou et al., 2011; Calvert et al., 2014, Lecours et al., 2017a; Lecours at al., 2017b).

The seafloor features have been recognized and grouped, taking into account the process that generates them (Fig. 2): (i) erosional features (identified by BPI), (ii) depositional features (identified by ruggedness and backscatter), (iii) anthropogenic structures (rip rap identified by ruggedness and backscatter and dredging areas by BPI) and (iv) biogenic features (identified by ruggedness). All submerged morphologies (bedforms) were first manually segmented and then automatically classified using terrain attributes. Most of the features are recognizable in the DEM, but some morphologies show a characteristic signal also in the backscatter mosaic.

3.2.3 Backscatter classification

Being a first-order proxy of seafloor substrate type, backscatter mosaics have been widely used to characterize the seafloor in terms of its abiotic and biotic components ultimately producing thematic representations of the seafloor composition (e.g. Brown et al. 2011; Diesing Rattray et al., 2013; Hasan et al., 2014; McGonigle and Collier, 2014; Ierodiaconu et al. 2018, Montereale-Gavazzi et al. 2018)

The goal of the backscatter classification is to divide the study area in sub-regions with homogeneous superficial composition. Several approaches have been proposed in the literature. A first issue in the classification is the choice of the number of classes and clustering methods. In this study, Jenks' optimization method was used to classify the backscatter data. This method provided good results in a previous study in the Venice Lagoon (Montereale Gavazzi et al., 2016). The Jenks' Optimization clustering is an automatic tool implemented in ArcGIS to classify rasters. Given a defined number of classes, the method seeks to reduce the variance within classes and maximize the variance between classes (Jenks, 1967). In our study area, we identified 4 different backscatter classes, taking into account collected sediment samples and backscatter signature.

3.2 Ground-truth data

The main goal of ground-truthing is to characterize the seafloor and validate the results of MBES acoustic data by means of direct observations. In this study, the ground-truth dataset is comprised of (i) surficial sediment grab samples and (ii) underwater images (from drop-frame camera). The position of the samples was provided by a GPS Seapath 300 with a Fugro HP differential Global Positioning System (0.2 m accuracy).

Based on sample depths and the angle of immersion of sampling devices, we estimate a maximum position error of 2.6 m. Therefore, to relate ground-truth samples with acoustic data, we averaged bathymetric and backscatter values over windows of 5 by 5 meters.

3.2.1 Sediment samples

A total of 44 surficial sediment samples were collected with a Van Veen Grab (5L) in two different research campaigns. The most recent samples (17) were collected in April 2014 (named N2-N23); the locations were selected to include all the characteristic textural patterns identified on the MBES datasets. To cover all the surveyed area, we decided to add another 27 sediment samples collected in March 2012 during another research project. The latter are located at the seaside, arranged in a regular grid and named from N100 to N126. All samples were classified according to the Folk and Ward method (1957). using Gradistat statistical package (Blott and Pye, 2001) after the analysis by dry sieving (16 mm to 38 μm).

3.2.1 Underwater images (Drop frames)

A survey was carried out on January 2015 at 20 stations by means of a drop-frame camera (3 replicates for each station). The device consisted of an action camera (Go-Pro HERO-3) and underwater lights installed on an aluminum frame which could be easily dropped from the vessel. The underwater images were collected on the same points of a subset of April 2014 sediment samples. Some additional stations were chosen to investigate particular seafloor features (e.g. seagrass patches, rip-rap seabed, etc.).

Representative still images (22.5 x 30 cm) were extracted from each recorded video and characterized in terms of biotic and abiotic features. Epimegabenthos (both living specimens and empty shells) were identified and counted. A total of 60 images were analyzed.

4. Results

4.1 Bathymetry and seafloor features classification

The measured bathymetry ranges from -30 m to -1 m. The shallower depths (> -2 m) are located inside the lagoon, near the harbor of Chioggia and the mudflats located in south-west part of the survey area. Conversely, on the seaside we observed greater depths especially on the north-east sector. However the greatest depths (< -15 m) are within a large scour hole (about 30 m deep) located at the west entrance of the inlet channel. The inlet channel depths vary from -14 m to -9 m, but in the south-east part where the channel connects to the sea, depths are shallower because of the presence of a sand deposit.

The seabed of the study area was predominantly flat or gently sloping: generally, the slope had a constant value of 1°, increasing up to 20° in correspondence to the major dune features. Only scour holes and anthropogenic artifacts showed a larger gradient up to 30° and 80°, respectively).

By the combined analysis of the MBES and ground-truth data, seabed features were classified (Fig. 3) in: (i) erosional, (ii) depositional and (iii) biogenic.

4.2.1. Erosional features

Scour holes are localized erosional features produced over a sediment surface in a turbulent current (Madricardo and Rizzetto, 2018). These features are readily identifiable in the bathymetric model and are characterized by various shapes and depths (Fig. 3a, 3b). Four scour holes have been identified, covering a total area of 294’371 m^2 (the 3.02 % of the study area).

The deepest scour is located inside the lagoon basin, near the inlet entrance and Chioggia harbor (Fig. 3a, 4a). Its shape is highly irregular, with maximum relative depth of 20 m and a surface of 119'084 m^2. The deepest point reaches about -30 m, with a slope ranging between 10° and 30°. This scour hole borders the stone-revetment area at the west side of the mobile barrier system (MoSE). The shape of the scour is indeed abruptly interrupted by the presence of concrete foundations (Fig. 3a upper right). Inside this bedform we collected a poorly sorted *gravelly sand* (N18 in Fig. 1) with a D50 of 243.00 µm, composed in large part by shell fragments and inorganic clasts > 2 mm. The comparative drop-frames show a sandy seafloor entirely covered by *Ophiothrix* sp.

Another two different scour holes were mapped at the breakwater tips (Fig. 3b, 4b): the scour at the northern tip presented an almost ellipsoidal shape with the main axis 500 m long directed almost parallel to the tidal inlet channel axis. It has a surface of 83'022 m^2 and a maximum relative depth of 3 m. Within this feature, we collected a well sorted *slightly gravelly muddy sand* (N110) with a small D50 (67.30 µm).

The scour hole at the southern breakwater tip has a smaller surface (53'387 m^2.) and an oval elongated shape with the main axis 452 m long. It is roughly oriented north-south and it has a relative depth of 4 m. The slope profile is quite irregular, with several steps, likely connected to collapses slumping processes due to steep and unstable sides.

These two scours were not present before the construction of the breakwater started in 2003, as it can be seen in Villatoro et al. 2010. Removing the bathymetry associated with these two scour holes and interpolating the remaining surface, we calculated that about 430,000 m^3 of sediments have been eroded in about 8 years.

A fourth scour hole (Fig. 4c) was identified at the seaside end of the inlet channel at the tip of the northern jetty with an irregular area of 38,900 m^2 and a relative depth of 2 m. It is almost parallel to scour 2.

Pools are distinct depressions of the seafloor whose origin is strictly connected to hydrodynamic processes (Klaucke and Hesse, 1996): inside a channel, near the curve, the current erodes the longest side, eroding the seabed. The pools are similar to scour holes, nevertheless the shape is more distinct (ellipsoidal) and the relative depth is lower (Fig. 3c). We identified pools exclusively inside the lagoon, especially in the northern part (channel-river dynamics). They occupy a total surface of 31’745 m^2 (0.33 %).

4.2.2. Depositional Features

Dune fields occupied 3.94 % of the study area (383’943 m^2). They result from the deposition of sandy and muddy sediments and are transversely arranged, according to the main direction of the current (Ashley, 1990). We found a total of 38 dune fields with wave length ranging from 2 m to 100 m and height from 0.02 m to 2 m, mainly small size 3-dimentional dunes but with occasionally large dunes localized near the inlet’s ends. They obey the relationship $\lambda = 0.79 * h - 1.13$, very similar to the Flemming equation (Flemming, 2000). No symmetric dune fields where found in the study area, indeed also the smallest dunes are slightly oriented toward sea, according to ebb tide. Though a single tidal cycle can influence the smaller dunes orientation, this is not true for bigger dunes whose orientation is determined by the direction of the residual currents and not by the currents of a single tidal cycle.

The biggest dune field observed is composed of very large dunes (H = 2.5 m, λ = 110 m) located at the inlet entrance close to the southern jetty (seaside) at a depth of

10 m and it covered about one half of the navigation channel (Fig. 3e, 5b). These dunes are 180° out of phase and considerably asymmetric, clearly oriented toward the sea (from west to east); on the stoss side the slope is about 1.2°, while on the lee side it is 20°. These characteristics suggest a predominant influence of the ebb tide current, with a consequent seaward sediment transport. Furthermore, over the stoss side, some smaller dunes are superimposed (H =20 cm, λ = 4 m). A ground truth station (N11) was located over the southernmost dune, where we collected a moderately sorted *slightly gravelly sand* (D50 = 54.1 μm). The drop-frame shows a homogenous sandy seafloor, with a low presence of shells and small superimposed ripples.

Two other very large dunes, which connected to form a U-shape, were identified north of the biggest scour hole, close to inlet entrance (lagoon side) at a depth of 6 m (Fig. 3f, 5c). Their wavelength is 100 m and their height is 2 m. These dunes are slightly asymmetric, developing in a northwest-southeast direction, with a stoss side slope of 1.2° and a lee side slope of 22°. Small dunes (H =10 cm, λ = 3 m) are superimposed on the stoss side. Close to these dunes, a grab sample was collected (N10): the sediment is a very poor sorted sandy gravel (D50 = 653.2 μm). The drop-frames show a sandy seafloor heavily covered by shells fragments. The backscatter classification suggests that the large dunes are covered by the same sediment found in the sample.

Point bars are depositional features that form inside the channel's bend and rivers below the slip-off slope (Hickin, 1974). Some sectors of the lagoon channels are frequently dredged to allow navigation. For this reason, we identified only one point-bar, located in the north part of the lagoon, in correspondence to a pool morphology (Fig. 3g) with a surface of 40'046 m^2 (0.41 %)

Ebb and flood tidal deltas are two typical morphologies of tidal inlets. These features are deposits of sediments (usually sand and mud) whose genesis is connected to the interaction of tides and alongshore transport on the coast and the shape depends on currents, waves, sediment supply, etc. (Hayes and Fitzgerald, 2013). The identified ebb-tidal delta occupies about 1.85 km^2 (19.01% of the total survey area). The flood-tidal delta, surface of 69’018 m^2 (0.71 %) is instead less distinguishable and its extent was not fully captured by the survey (Fig. 3).

4.2.3. Anthropogenic features

Rip-rap is composed of rocks used to build the anthropogenic hard structures as breakwaters, jetties, armored shorelines, etc. (Pister, 2009). The presence of these features is increasing in the world to manage sea level rise and erosion. They usually host a particular habitat and could alter surrounding areas (Bulleri and Chapman, 2010; Dafforn et al. 2015, Perkins et al. 2015, Aguilera et al. 2017). In the survey area riprap seafloors were mapped around breakwater and near jetties. Riprap was observed also in proximity to the mobile barriers where the seafloor has been has been “armored” to protect the trench from the bottom sediment transport. These features have an irregular profile and are in relief from the bottom (Fig. 3h) and occupies a total surface of 525’937 m^2 (5.39 %).

Dredging marks can be distinguished by the sharp vertical gap and the reprofiling tools incisions. The dredging sites may have important consequences for ecosystem functionality due to direct hydrodynamic and morphology alterations (Cozzoli et al., 2017). In this study, these features occupy a surface of 111,483 m^2 (1.14 %). The marks are clearly visible only in very shallow water. The depth of the excavation is variable, but generally is about 2 - 2.5 m (Fig. 3i).

Mobile barriers (MoSE) allocation started only in 2015 and will probably finish at the end of 2019; the trench is easily identifiable by the regularity of its shape (Fig. 3j). It covers a surface of 23’190 m^2 (0.24 %) and shows a mean vertical dimension of 10 m.

4.2.4. Biogenic features

Seagrass patches are identifiable as speckled round/ellipsoidal shapes, slightly highlighted (Fig.3k). These natural features are located in the south-west margin of the lagoon area, at a depth of 2/2.5 m and occupy a limited surface area, 13,168 m^2 (about the 0.14% of the study area). The observed patches are *Cymodocea nodosa* meadows. The up-to-date seagrass distribution over the Lagoon of Venice mudflats is reported in Curiel et al. (2014).

4.3 Ground truth samples analysis

4.3.1. Sediment samples

We analyzed a total of 44 samples, subdivided between open sea, lagoon and inlet channel (tab 1). The range of median diameters is broad and change from 60.3 μm to 2.9 mm. Most of the sediment grain size were inside sand class. In detail, *slightly gravelly sand* is the predominant size class. Gravelly materials were also found (with 3 *sandy gravel* samples). Only 2 samples were in mud class (*slightly gravelly sandy mud*). On the seaside, there is always a high percentage of sand and also frequently abundant mud. Instead, inside the inlet there is less sand and more gravel. Inside the lagoon, mud samples were found near the shallow water salt marshes, while gravelly samples were located at greater deeps (e.g. inside dredged channels).

Several samples contained an abundant coarse fraction (> 2 mm) which is not typical of a coastal lagoon systems.. This coarse fraction consisted of bioclastic grains, mostly shells fragments, especially belonging to bivalve or gastropod mollusks. Other organic material, like wood pieces, was present in low quantities, except for N5 (see Fig. 1 for the sample location). Also, non-bioclastic grains were not very abundant, except for N18.

Sorting of the sediment samples is strongly dependent on the site of collection within the study area. All seaside sediments are well-sorted or moderately well-sorted, except for sample N100 which was poorly-sorted. On the contrary, inside the lagoon and along the inlet channel the sediments show a high degree of variability, with the sorting index varying between very poorly-sorted to well-sorted. The least sorted samples consisted of sediments with a lower content of sand: where mud or gravel is abundant the grain size variability is larger; indeed, the very poorly-sorted samples (N2, N6, N10 and N12) are sandy gravels or gravelly sands. Where the content in sand is higher, usually the sediment is well sorted.

4.3.2. Seafloor images

Several benthic taxa, mainly epimegabenthos, characterizing the various habitats (both alive specimens and empty shells) were recognized from underwater images (Appendix B). Although some species were identified with high abundance, the number of observed taxa remains relatively low, summing to a total of 37. With the exception of some seagrass patches (*Cymodocea nodosa* (Ucria) Asch), easily recognizable also from MBES data, observed in the western margin of the lagoon side, and red/brown algae colonizing the central inlet rip-rap, the seabed lacks of macrophyte cover.

In 11 out of 19 stations we observed live organisms, most commonly *Carcinus aestuarii*, *Nassarius nitidus*, Actiniaria and Paguroidea, mostly on sandy/muddy sediments and over seagrass meadows. The stations with coarse sediment and shell fragments presented a lower number of live organisms. In the deepest stations, N18 and N23 (Fig.1), characterized by boulders or pebbles, a large number of *Ophiothrix* sp. covered the seabed.

Empty shell remains belonging to the thanatocoenosis were identified in 14 out of 19 stations, mostly Bivalvia, and in particular Veneridae. We also identified very frequently Mytilidae, Pectinidae and Ostreidae. Among gastropods, we mostly observed *Nassarius nitidus* and *Bittium* sp.

4.4 Backscatter classification

The collected backscatter ranges from -68.54 dB to 4.64 dB; some outliers (visibly associated with artifacts) are probably connected to errors during registration or conversion. The backscatter data are characterized by a Gaussian distribution, with a mean of -24.20 dB and a mode of -25.85 dB. The associated standard deviation is 3.22.

Using the Jenks' optimization method, we have obtained 4 BS classes (fig. 6), where the classes are: very low signal: < - 28.07 dB (SGMS_MS_SGSM); medium-low signal: -28.07 ÷ -24.63 dB (S); medium-high signal: -24.63 ÷-20.90 dB (SGS); very high signal: > -20.90 dB (SG_GS). The classes were identified with an overall accuracy of 75%.

4.5 Backscatter classification accuracy

Many measures exist to verify the accuracy of a classification process. One of the most popular is deriving the confusion matrix and count the percentage of correctly allocated cases (Foody, 2002). This technique, created for land using research, gives the ideas of accuracy using two different point of view, user's and producer's accuracy, depending on if the calculation process is based upon the matrix rows or columns (Story and Congalton, 1986). Furthermore, an overall accuracy can be derived from these tables.

The unsupervised Jenks' classification shows an overall accuracy of 75%, identifying correctly 33 stations on 44 totals (Tab. 1). The used method achieved reasonable accurate predictions of coarser sediments (SG_GS and SGS classes). However, Jenks' does not reach a sufficient accuracy for the classes S and SGMS_SM_SGSM: in particular, the class S are much more attributed to the seafloor than what it really is. We can only speculate that the false stations are probably located in unclear backscatter patches, where there is coexistence of classes. The low accuracy could also be related to the low number of collected grab samples of this seafloor types. For the class SG_GS, despite having few samples, the backscatter values are quite major to the other classes and this permits a correct classification of the seafloor inside this class.

However, a limitation of our study is that we used only a pixel-based classification method and different solutions (e.g. OBIA) must be tested to make more reliable the classification.

4.6 Benthic habitat classification

Benthic habitat classes have been identified based on the backscatter, the terrain attributes, the sediment samples and the underwater images from the ground-truth stations (Figs. 7 and 8). Each benthic habitat is characterized by specific biotic features specified in the description of Fig. 7.

Habitat classes are generally described by the sediment composition, which influences the backscatter signal. The habitat classes, i.e. *Coarse shell detritus*, “Sand with sparse shell detritus”, “Bare sand” and “Muddy sediment” at the seaside were defined using the backscatter classification supported by the sediment samples data and the classified seafloor images (Figs 7 and 8).

However the information from the backscatter intensity alone can sometimes not be enough to differentiate all target habitats (see e.g. De Falco et al., 2010; Lucieer et al., 2013).

In our case we isolated the habitat classes “*Artificial rock bed*” and “*Seagrass meadows*”, also using morpho-bathymetric attributes, like bathymetry itself and ruggedness (Fig. 2). The “*Artificial rock bed*” presented indeed very high ruggedness values and a distinctive backscatter pattern characterized by chaotic patches, whereas “*Seagrass meadows*” were visible in the bathymetry and showed medium to high ruggedness values confined in circle/oval shapes.

The class “*Lagoon mudflat*” was defined using both the classification of the backscatter and of the seafloor features: the lagoon area with lowest values of backscatter, as well as the tidal point bar and flood tidal delta were grouped into this habitat class.

4.6.1 *Class 1 – Coarse shell detritus*

The main feature of this habitat is the thick layer of biogenic detritus composed of coarse shell fragments which covers completely the bottom, masking the underlying sediment. The shells can have a different degree of cementation and variable fauna colonization. The associated textural group is usually sandy gravel, with very high D50 and very poor sorting. Mud content is typical missing. Coarse shell detritus is very variable in terms of species composition: it included mostly bivalves such as *Chamelea gallina*, *Venerupis aurea*, Mytilidae indet., Ostreidae indet. and Pectinidae indet., but also gastropods, sea urchins (class Echinoidea) and decapod remains. Occasionally, the brittle star *Ophiothrix* sp. is very abundant and completely cover the bottom. Observed living organisms include some bivalves and hermit crabs (Paguroidea indet.). Moreover, the coarse and partly cemented detritus behave as a hard substratum allowing the colonization by epibionts such as Actiniaria indet. and Serpulidae indet. Sometimes macroalgae (*Ulva* sp.) and seagrass fragments are observed.

This class occupies 821,693 m^2, i.e. about the 8.42% of the study area, and is placed especially along the inlet and in the northern part of the lagoon, while in the open sea it is less represented. Moreover, these seafloor types are frequently located near riprap and it is sometimes difficult to distinguish them due to similar backscatter and ruggedness values. This habitat is often found in relation to specific features and underlying hydrodynamic processes seem to be responsible for their distribution. In detail, this substratum often fills concave morphologies (i.e. scour holes and pools). It is not completely clear if these bioclastic debris are transported by the currents from the surrounding area or if they are a deep ancient sediment subsequently exposed by current erosion. This kind of seafloor cover is usually related to high backscatter value due to the strong reflectivity of shells (Stanic et al., 1988; Yu et al., 2015).

525 4.6.2 *Class 2 – Sand with sparse shell detritus*

526 This is the most abundant habitat in the survey area with a surface area of 4,495,740 m^2 (≈ 46.05 %) and is distributed almost everywhere, except along the inlet. Slightly gravelly sand group dominates the substrate type of this class. High percentages of bioclastic detritus (mostly mollusc shell fragments) are often present. Mud content is low. The sorting is usually moderate. The most common cast shells remains include *Bittium* sp., *Chamelea gallina*, Solenoidea indet. and Mytilidae indet. Alive individuals of *Asterina gibbosa*, *Carcinus aestuarii* and *Nassarius nitidus* have been observed. Furthermore, this class is often connected to various seafloor features (dune fields, scour holes and pools). These surfaces are related to medium to high values of backscatter, basically depending on the shell density.

537 4.6.3 *Class 3 – Bare sand*

538 This is the second largest habitat class in the study area with 3,105,818 m^2 (≈ 31.82 %) and it is located almost exclusively in the marine part. The associated sediment is consistently sand, with very low percentages of other fractions. The underwater photos show a bare homogeneous seabed, with very well sorted sands usually arranged in small ripples (few centimeters of height). There is a paucity of benthic fauna and vegetation cover. Biogenic detritus is typically missing. This habitat is usually not connected to any large bedform and the backscatter signature is medium to low.

547 4.6.4 *Class 4 – Lagoon mudflat*

This class includes all the mudflats located inside the lagoon basin (e.g. Sarretta et al., 2010) and occupies 206,002 m^2 (≈ 2.11 % of the study area). The typical depth associated to this habitat are lower than 4 m, with the only exception of mudflat regions around lagoon scour holes that reaches about -8 m. The backscatter signature is often low, but patches with medium-high backscatter are sometimes observed due to the presence of shells deposits or dredging channels this habitat is located also on the tidal point bar and flood tidal delta located in the area. The collected samples are very well sorted muddy sediments, with poor presence of shells. These muds are very dense and with a plastic consistency. Observed taxa include lagoon vagile epifauna (e.g. *Carcinus aestuarii* and *Nassarius nitidus*) and significant vegetation cover occurs (mainly *Ulva* sp.). Furthermore, a cover of benthic diatom film is frequent.

4.6.5 Class 5 - *Muddy sediment*

Thie *Muddy sediment* habitat occupies 582,265 m^2 (≈ 5.96 % of the survey area). It is distributed mainly on the marine side of the study area, parallel to the coastline and starting at a depth of about 14 m. This habitat the mud belt found along the Venetian coasts due to the sediment input from the rivers (Albani, 1988). The substrate in this class is mostly well-sorted muddy sands or sandy muds, with low D50. The percentage of shells fragments is often very low. A cover of benthic diatom film is frequent. This class has a high number of observed species, including in some cases macrophytes. Noticeably, *Ulva* sp. is found on the marine side, either free floating or attached to the thanatocoenosis. Observed zoobenthic taxa include both infauna (e.g. *Echinocardium cordatum* and Veneridae) and vagile epifauna (e.g.

C*arcinus aestuarii*). This is the class with lowest backscatter intensity, clearly indicative of fine sediments. No bedforms are associated with these seafloors.

4.6.6 Class 6 – *Artificial rock bed*

This habitat class, that occupies a surface of 537,045 m^2 (≈ 5.50 % of the study area), corresponds to the seafloor covered with rip-rap. It is distributed along the jetties, the breakwater and in the middle part of the inlet, where boulder revetments have been placed to defend MoSE trench. This class often coincides with the borders of the surveyed area, due to shallow water constraints to the navigation. The underwater images show an irregular seabed with numerous boulders (tetrapods) alternate with muddy sediment patches. A thick layer of bioconcretion, mostly oysters and tube-building worms belonging to Serpulidae, covers the rocky surfaces. Macroalgae such as *Ulva* sp. are also present. *Ophiothrix* sp. is present in high number, sometimes covering the entire available surface. Poorly sorted sandy mud, with the presence of several encrusted shells, has been collected from the small patches among the boulders. The backscatter values associated to this habitat is not uniform and it does not clusterize, due to the alternate presence of rocks (strong backscatter) and muddy patches (low backscatter). Probably the abundant biological coverage is also influencing the backscatter signature (De Falco et al., 2010; McGonigle and Collier, 2014). For this reason, ruggedness has been used to identify the habitat.

4.6.7 Class 7 - *Seagrass meadow*

This habitat class, the smallest in the survey area occupying only 13,152 m^2 (≈ 0.13 %), represent the seabed with seagrass cover. It is located inside the lagoon, at depths lower than 3 m, near Chioggia harbor. The species is *Cymodocea nodosa* (Ucria) Ascherson, which, together with *Zostera marina* L. and *Nanozostera noltii* Hornemann, make up most of the seagrass prairies over the Venice lagoon (Curiel *et al.*, 2014). The collected images show a well sorted fine sediment seafloor with seagrass patches, some shell fragments and macroalgae, such as *Ulva* sp. The recorded benthic community, both vagile and sessile, is often abundant. Also, in this case, ruggedness has been used to identify

4.7 Anthropogenic objects

The analysis of high resolution bathymetry (0.2 m) allowed the visual identification of punctual anthropogenic objects placed voluntarily or not on the sea bottom. We mapped a total of 541 objects, grouped into 7 different categories (Fig. 9). The most common described objects are *Rip-rap debris* and *Bricola* (wooden poles used to delimit the navigation channels) (in yellow and grey in Fig. 9, respectively). Most of the objects were found inside the lagoon and along the inlet channel and close to the breakwater, whereas the deeper sea area presented less objects. *Tire* (in blue in Fig. 9), commonly used as fenders by boats, and *Bricola* elements were localized exclusively inside the lagoon, whereas in the deeper sea area *Rip-rap debris* prevailed. We found a total three wrecks (in purple in Fig. 9) inside the lagoon and in the inlet channel. The bathymetry highlighted the presence of a few cables and poles (in red and light blue in Fig. 9) on the seafloor.

5. Discussion

5.1 Tidal inlet seafloor features and sediment distribution

The construction of the seaside breakwater, built between 2003 and 2006, most likely significantly changed the hydrodynamic configuration of the flow as predicted by Ghezzo et al., 2010. The changes are schematically summarized in Fig 10.

Indeed, the water outflowing jet splits into two jets: the main one with direction west-east and a secondary that heads south. Indeed, the narrowing of the inlet section designed to provide space for auxiliary MoSE infrastructures, i.e. navigation locks and refuge harbours, altogether increased the flow velocity (Ferrarin et al., 2015 and references therein) (Fig. 10). As a direct consequence, a general coarsening of the sediment distribution seems to have occurred inside the inlet channel (Figs. 8, 10). By comparing our classified BS maps with the results described by Villatoro et al. (2010), we found a jet of gravelly sediments exiting the inlet channel that was not present in 2008 (Figs. 8, 10). The only areas with a finer sediment are located in the southern lagoonal part of the study area and in the area protected by the breakwater outside the inlet (yellow and red classes in Fig. 8). Over the residual ebb-tidal delta, we find predominantly Sand with sparse shell detritus (light blue in Fig. 8) whereas sandy and fine sediments are dominant in the seaward side of the study area (orange and red classes in Fig. 8).

The three scours shown in Fig. 3a and 3b have different sediment distributions: the backscatter of the scour at the lagoon side (Fig. 8) shows the presence of different sediment types: coarser at the scour northern side (classes *Coarse shell detritus* and *Sand with sparse shell detritus*) and finer at the scour southern side (*Bare sand*). Within the scours at the breakwater's tips (Fig. 3b) the backscatter signal highlights the presence of mainly *Sparse shell detritus* (Fig. 5).

The presence of the gravel fraction, i.e. shell detritus, could be related to a) the deposition of shells transported by the currents from the area surrounding the scours, or b) the erosion of a deep ancient fine sediment rich in organic detritus buried by the ebb tidal delta, leaving the coarser and heavier shells at the bottom of the scours.

The internal lagoon scour is considerably older than the breakwater scour holes and its presence is documented already by the historical military hydro-topographic map of Denaix of 1810 ca (Magrini 1933). The sediment distribution is likely related to the action of the currents which is stronger in its northern part, whereas its southern part is closer to an area of deposition, rich in muddy sediment.

Likely, these depressions eroded the deep silty clayey sediments at the ebb –tidal delta basis (sample N110). This material could also belong to the prodelta Holocene sediment facies deposited in a marine –lagoon environment with abundant fresh water inputs coming from a paleo-river Brenta (Zecchin et al., 2008). During marine transgression events, the river delta moved several times. Zecchin et al. (2008) found this sediment at a depth of 15-20 m in the core L1 –CNR collected in the area now occupied by the breakwater.

Scour holes around breakwaters have been observed globally (e.g. in Japan- Sato et al. 1968, Katayama et al., 1974; in The Netherlands-Delft Hydraulics, 1988; in the U.S.- Lillycrop and Hughes, 1993). Processes leading to the formation of scour holes around hard coastal structures have been extensively studied mainly on the basis of tank experiments (Sumer and Fredsøe, 1997; Fredsøe and Sumer ,1997; Sumer et al., 2001; Noormets et al., 2006). Fredsøe and Sumer (1997) investigated in a tank experiment the scouring at the round head of a rubble-mound breakwater (similar to our case) using regular waves. They found that the major mechanism responsible for the scouring was the formation of lee-wake vortices in each half period of the waves. The scouring process, governed by the Keulegan-Carpenter number, *KC*, depends on the base width B of the breakwater head and the width of the protection layer L on the seafloor. Larger values of *KC* imply the forming of larger scour holes. In our case with B=60 m and L=40 m, we obtained *KC* =1.14 from the relation $KC = 1 + (\frac{L}{1.75B})^2$ (eq. 6 of Sumer and Fresøe (1997)). This value of *KC* corresponds to a separated flow regime with no horse-shoe-vortex formation in front of the breakwater. In this flow regime, a lee-wave vortex forms close to the structure in every half period of the motion (Sumer and Fresøe, 1997). The depth of the scour holes were likely substantially enhanced by the presence of co-directional currents that contribute to the wave action. In this setting, large-scale vortices generated at the breakwater tip could increase the transport capacity of the flow (Fig. 10). To fully understand the role of currents and waves in the scouring process, however, a 3D hydrodynamic and sediment transport modeling analysis would be required.

Most dune fields fall inside the classes *Coarse shell detritus* and *Sand with sparse shell detritus*. Looking at the classified backscatter, however, it is possible to distinguish a repetitive pattern of sediment distribution with the class SG_GS in the troughs and the class SGS over the crests (Fig. 11). This sediment pattern is related to the larger energy that is necessary to remove the coarser sediment from the troughs (Fig.11). Feldens et al. 2014 found higher side-scan sonar backscatter intensities between dunes in the dune fields close to the Fehmarn Island in the south-western Baltic Sea in water depths between 12 m and 23 m. In deeper waters between 60 m and 110 m, on the outer Murcia continental shelf (western Mediterranean Sea). Durán et al. (2017) found that the backscatter imagery of a dune field extending from Cape Cope to the Aguilas submarine canyon displayed higher intensity values on the crests and lower intensity values on the troughs. The different sediment pattern could be related to the bi-directional nature of the tidal flows in the case of the Chioggia inlet and to the flow reversal within the Fehmarn Belt in the Baltic Sea or possibly to the combined action of the waves and currents. A similar anti-correlation between bathymetry and backscatter values is found also for a sand waves field in the Cook Strait in New Zeeland (Lamarche et al., 2011).

The relationship between the wave length and height of the identified dune fields is consistent with the empirical relationship found by Flemming (1988). In our case $\lambda = 0.79 * h - 1.13$, where λ is the dune wave length and h the dune height with the correlation coefficient $R^2 = 0.84$.

5.1 The anthropogenic impact on tidal inlet benthic habitats

The human influence on the coast is stronger than in other regions of the Earth given that more than 40% of the world population lives in coastal neighborhood (Small and Nicholls, 2003, Ouillon, 2018). It is indeed recognized that human activities can be a morphogenetic process (Marriner et al., 2012; Kołodyńska-Gawrysiak and Poesen, 2017; Poesen, 2018) and can influence the main characteristics of an estuarine environment such as the tidal prism (Kerner, 2007; Winterwerp et al., 2013), the turbidity (Rapaglia et al., 2011; Winterwerp et al., 2013; Rodrigues et al., 2018), the sediment budget (Syvitski et al., 2005; Sarretta et al., 2010; Wang et al., 2015; Zhu et al., 2016), the erosion rate (De Roo and Troch, 2014; Zaggia et al., 2017) and the morphodynamics itself (Jeuken and Wang, 2010; Monge-Ganuzas et al., 2013).

The Chioggia tidal inlet represents an example where human-induced morphological processes have radically changed the seafloor over time. By comparing the bathymetric data collected in 2013 and the last complete bathymetry of the lagoon collected in 2002 (Magistrato alle Acque, 2002), we observed three main processes ongoing in the Chioggia inlet (Figs. 10, 12): a) the main inlet channel experienced severe to extreme erosion likely due to the increased flow (Fig. 12), and in some parts of the inlet channel the deepening was due to the dredging and the seafloor armouring associated with the MoSE constructions (Figs. 2, 3i and 3j and 10 e 12); b) a strong deposition occurred in correspondence to the flood tidal delta (Figs. 3 and 12), the large dunes (Figs. 3e, 3f and 12), the large hard structure scour hole (Figs. 3a and 12). Likely there was fine sediment deposition in the area inside the breakwater where we found muddy sediments; c) large scour holes were created around the breakwater tips that were not present before the breakwater construction as documented by Villatoro et al. (2010).

As observed by Sarretta et al. (2010), there is a diffuse erosive process in the central and Venice Lagoon, with consequent sediment transport to the inlets. The lagoon southern sub-basin related to the Chioggia inlet is less affected by this process, which is stronger in the Malamocco area (Saretta et al., 2010). Still, it is possible that part of the eroded sediment from the lagoon is transported to the Chioggia inlet, partly depositing on the flood tidal delta, on the large dunes and in the internal hard structure scour hole and partly transported outside the inlet.

We observe that the seabed composition in the study area is extremely heterogeneous, ranging from sandy gravels to sandy mud, but with a general predominance of sandy substrata. The fine sediment is abundant on the very shallow waters in the South-West area close to the city of Chioggia and in the open sea, whereas the coarse sediments, composed by shell detritus, are copious along the inlet and in the main navigation channels. Coarse shell detritus patches are known to be locally present in the Venice Lagoon, and have already been mapped by Montereale Gavazzi et al. (2015) in the bed of the Scannello Channel.

Within the tidal channel inlet, the erosive process already observed in 1927 (Villatoro et al., 2010) is still active (Fig. 11). The resizing of the inlet channel and the dredging operations within the MOSE project are very likely responsible for the deepening of the channel and a general increase of the current velocities inside the channel inlet, as already foreseen by the modelling study of Ghezzo et al. (2010). Villatoro (2010) found a deposition trend in the final part of the inlet closer to the southern jetty (from -10 m in 1927 to -4 m in 2006). The 2013 measures however show a new erosive trend in that area.

By comparing with the sediment distribution of 2006 by Villatoro et al (2010), we observe that the grain size of the inlet seafloor has increased with dense shell detritus deposits often present in the study area.

In the sea side area instead, the ebb tidal delta started to form after the end of the jetties construction, continuing its deposition process for half a century (Brancolini et al., 2006). After the construction of the breakwater (2003 – 2006), however, just a few years were sufficient for an important erosive process to begin and to form large scours at the two breakwater ends. Furthermore, these scour holes could even endanger the stability of the breakwater itself by undercutting its base. Besides, the load of the new structures that will support the MoSE has increased the subsidence rate, showing a deepening up to 40 mm/year in some emerged sectors of the inlet (Tosi et al., 2012). We can speculate that soil settlement influences also the bathymetry of the seafloor.

The described benthic habitat classes are characterized by specific seafloor composition and morpho-bathymetric attributes, strongly dependent upon hydrodynamics and sediment budget. These are major ecological factors for the highly dynamic lagoon inlets, influencing other factors, such as bedload transport as well as suspended sediment transport and deposition, oxygenation, saprobity, etc., which overall reflects on benthic communities recruitment, structure and functioning:. hydrodynamic alteration can therefore strongly modify benthic habitats and communities and their natural succession (e.g. Ashley and Grizzle, 1988; Blanchet et al., 2005; Pranovi et al., 2008; Tagliapietra et al., 2012).

Most of the observed habitats, as well as their general spatial succession from the lagoon seawards, are well documented for the Lagoon of Venice and the adjacent coastal area, even though they are generally described in terms of their abiotic features, i.e. sediment composition or biocoenosis (Vatova, 1940; Vatova, 1949). The same general pattern is expected to be replicated at the other two lagoon inlets. *Coarse shell detritus* habitat has been observed on tidal channels seabed also in more internal parts of the Venice Lagoon (Montereale Gavazzi et al., 2015).

We observed a human-made habitat class, here named *Artificial rock bed*. This hard substratum habitat class, that occupy about 5.50 % of the study area and is found in correspondence to jetties and rip-rap, hosts a diversified and structurally complex biological community, very different compared to the adjacent habitats. In fact, nearly all the hard substrata in the west coast of the northern Adriatic sea are artificial. The recent works at the inlets have greatly increased the previous extent of this habitat, in particular by filling a 400 meters long section of the channel seabed continuously from side to side.

Several studies have been carried out globally on artificial reef habitats, which are a consequence of increasing human coastal urbanization and coastal protection from sea level rise and should be considered a main driver of change in coastal environments (e.g. Chapman, 2003; Bulleri and Chapman, 2004; Pister, 2009; Bulleri and Chapman, 2010; Perkins et al., 2015). However, they do not necessarily represent a negative impact on the ecosystem. Artificial hard substrata over a otherwise soft-sedimentary seabed increase habitat heterogeneity, therefore enhancing biodiversity (Turner, 1989; Williams, 1964). They increase the surface area of the substratum and spatial complexity for benthic communities (Svane & Petersen, 2001) and play as refugia, feeding grounds and nursery area for fish populations (Brickhill et al. 2005; Clynick et al. 2007). However, their ecological functioning may differ consistently from natural rocky habitats (e.g. Ferrario et al., 2016) or from the pre-existing sandy bottom. The way these infrastructures are designed, and the way they are related to surrounding habitats, is central to their ecological effects (Bulleri and Chapman, 2010). Despite the artificial rock bed recently deployed on the inlet seabed, it may be considered not to be particularly extended compared to the other habitats, impacts related to habitat fragmentation and loss of connectivity cannot be excluded. Moreover, artificial substrata may promote the settlement of non indigenous species in comparison to soft-sedimentary environment (Wasson et al., 2005), even though artificial rocky structures may behave in a comparable way to natural reefs (Glasby et al., 2007). This issue deserves particular attention given the status of the Lagoon of Venice as the main hotspot for non-indigenous specie within the Mediterranean Sea (Occhipinti-Ambrogi et al., 2011). More ecological research is needed to verify the ecological role of this habitat for the whole system and to understand its evolution.

Dredging is also responsible for significant ecological impacts (e.g. Van Raalte, 2006; Monge-Ganuzas et al., 2013; Van Maren et al., 2014). In many cases, this activity increased environmental deterioration, by changing the pattern of hydrodynamics, augmenting salinity stratification and resuspending muddy sediments, pollutants and nutrients (Newell et al., 1998; Teatini et al., 2017). In this study, we identified 111,483 m^2 of dredging surfaces (about the 1.14 % of the study area), located exclusively in the shallow lagoon basin.

Dredging can alter the natural development of the lagoon geomorphology and its equilibrium (Healy et al., 1996): for example, we mentioned that the west margin of the flood tidal delta is sharply cut for the presence of a dredging channel. This bedform that should develop an important and structured shape (Hayes and Fitzgerald, 2013) have been seriously resized to just 69,018 m^2. Furthermore, the presence of dredging channels near mudflat and salt marshes, can limit the spread of seagrass meadows, which are strongly dependent on the depth gradient (Paulo et al., 2016).

Finally, we quantitatively assessed the number and mapped the distribution of abandoned or lost objects on the seafloor grouping them in different recognizable categories. The anthropogenic submerged litter and abandoned fishing gears are an emerging issue for the society and for marine sciences: however, most of the available researches are based on photo/video surveys (e.g. Pham et al., 2014) or on samples collection with seabed trawling (Grøsvik et al., 2018; Kammann et al., 2018; Maes et al., 2018) being mainly focused on plastic/glass rubbles. This study shows that MBES surveys can be precious to map macro-litter distribution in shallow coastal areas.

6. Conclusions

In this study we mapped with unprecedented detail the morphology, the sediment distribution and the habitats of a tidal inlet strongly affected and modified by human activities. We found 10 types of morphological features and 4 sediment classes and described the sediment characteristics of each mapped morphology. We identified the sediment distribution within dune fields (with wave length and height ranging from 2 m to 100 m and from 0.02 m to 2 m, respectively), finding *slightly gravelly sand* on crests and *sandy gravel – gravelly sand* in troughs.

Through the combined analysis of MBES, grain size and seafloor images we identified seven different benthic habitats, among which *Sand with bioclasts* (46%) and *Bare sand* (32%) were the dominant classes. A new habitat, that we called *Artificial rock bed*, was found on the rip-rap revetment placed near the mobile barrier still under construction to protect the historical city of Venice and the other lagoon islands from floods.

We estimated that the new pattern of flow around these hard structures also caused the erosion of 430,000 m^3 of sediment in 8 years. A general coarsening of the sediment distribution seems to have occurred inside the inlet channel due to the narrowing of the inlet (MoSE construction).

The Chioggia tidal inlet represents an example where the seafloor has changed over time due to human interventions, therefore humans as a geomorphic agent and this study quantitative assessment of how anthropogenic intervention can modify the seafloor morphology and habitat, showing the direct and indirect consequences of the construction of new hard structures on morphodynamics. The multidisciplinary approach of this work can be applied to study the consequences of the substantial transformation of coastal landscapes that is taking place in response to urbanization and sea level rise. The proliferation of a variety of built structures (breakwaters, seawalls, jetties and pilings, etc.) and anthropogenic activities in the intertidal zone and near shore estuarine and marine waters calls for a comprehensive assessment of their impact on the seafloor for a knowledge-based management of the coastal environment.

Acknowledgments

The authors would like to acknowledge all the rest of the ISMAR Team (Federica Foglini, Aleksandra Kruss, Marco Bajo, Debora Bellafiore, Elisabetta Campiani, Valentina Grande, Lukasz Janowski, Erica Keppel, Elisa Leidi, Francesco Maicu, Vittorio Maselli, Alessandra Mercorella, Claudio Pellegrini, Antonio Petrizzo, Mariacristina Prampolini, Alessandro Remia, Federica Rizzetto, Marzia Rovere) that contributed to collect and process the MBES data of the Venice Lagoon in 2013 (available from http://dx.doi.org/10.1594/IEDA/323605). The author are grateful to the crew of the research vessel Litus for their skilful help during the survey and Loris Dametto for his technical help on the ground truth sampling. The authors would like to thank Christian Ferrarin for providing the tidal corrections for the MBES data and William McKiver for reading the manuscript. Finally, Stefano Fogarin would like is very grateful to Prof. Giancarlo Rampazzo of the University of Ca' Foscari for his help during his MSc thesis, when part of this work was carried out. This work was supported by the National Flagship Project RITMARE, funded by MIUR, the Italian Ministry of Education, University and Research.

References

Aguilera MA. 2017. Artificial defenses in coastal marine ecosystems in Chile: Opportunities for spatial planning to mitigate habitat loss and alteration of the marine community structure. Ecological Engineering.

Albani AD, Favero VM, Barbero RS. 1998. Distribution of sediment and benthic foraminifera in the Gulf of Venice, Italy. Estuarine, Coastal and Shelf Science 46(2): 251-265.

Amos CL, Villatoro MM, Helsby R, Thompson CEL, Zaggia L, Umgiesser G, Venturini V, Are D, Sutherland TF, Mazzoldi A, Rizzetto F. 2010. The measurement of sand transport in two inlets of Venice lagoon, Italy. Estuarine, Coastal and Shelf Science 87(2): 225-236.

Ashley GM. 1990. Classification of large-scale subaqueous bedforms: a new look at an old problem. Journal of Sedimentary Petrology 60: 160-172.

Ashley GM, Grizzle RE, 1988. Interactions between hydrodynamics, benthos and sedimentation in a tide dominated coastal lagoon. Marine Geology 82: 61-81.

Balletti C. 2006. Digital elaborations for cartographic reconstruction: the territorial transformations of Venice harbours in historical maps. e-Perimetron 1(4): 274-286.

Bird ECF. 1994. Physical setting and geomorphology of coastal lagoons. In Kjerfve, B. (ed.), Coastal Lagoon Processes.

Blanchet H., de Montaudouin X., Chardy P., Bachelet G., 2005. Structuring factors and recent changes in subtidal macrozoobenthic communities of a coastal lagoon, Arcachon Bay (France). Estuarine, Coastal and Shelf Science, 64: 561-576.

Blott SJ, Pye K. 2001. GRADISTAT: a grain size distribution and statistics package for the analysis of unconsolidated sediments. *Earth surface processes and Landforms 26*(11): 1237-1248.

Brancolini G, Tosi L, Baradello L, Bratus A, Donda F, Rizzetto F, Zecchin M. 2006. Preliminary results of the high resolution seismic surveys in the Venice Lagoon. Scientific Research and Safeguarding of Venice, 2004-2006.

Brickhill, M.J., Lee, S.Y., Connolly, R.M. 2005. Fishes associated with artificial reefs: attributing changes to attraction or production using novel approaches. Journal of Fish Biology, 67: 53-71.

Brown AG, Tooth S, Bullard JE, Thomas DS, Chiverrell RC, Plater AJ, Murton J, Thorndycraft VR, Tarolli P, Rose J, Wainwright J, Downs P, Aalto R. 2017. The

938 geomorphology of the Anthropocene: emergence, status and implications. Earth Surface Processes and Landforms 42(1): 71-90.

941 Brown, C.J., Smith, S.J., Lawton, P. and Anderson, J.T., 2011. Benthic habitat mapping: A review of progress towards improved understanding of the spatial ecology of the seafloor using acoustic techniques. Estuarine, Coastal and Shelf Science, 92(3), pp.502-520.

946 Bulleri F, Chapman MG. 2004. Intertidal assemblages on artificial and natural habitats in marinas on the north-west coast of Italy. Marine Biology 145(2): 381-391.

949 Bulleri F, Chapman MG. 2010. The introduction of coastal infrastructure as a driver of change in marine environments. Journal of Applied Ecology 47(1): 26-35.

952 Calvert J, Strong JA, Service M, McGonigle C, Quinn R. 2014. An evaluation of supervised and unsupervised classification techniques for marine benthic habitat mapping using multibeam echosounder data. ICES Journal of Marine Science 72(5): 1498-1513.

957 Carniello L, Defina A, D'Alpaos L. 2009. Morphological evolution of the Venice lagoon: Evidence from the past and trend for the future. Journal of Geophysical Research: Earth Surface, 114: 1-10.

961 Cavazzoni S. 1995. La laguna: origine ed evoluzione. La laguna di Venezia, Verona; 41-75.

Chapman MG. 2003. Paucity of mobile species on constructed seawalls: effects of urbanization on biodiversity. Marine Ecology Progress Series 264: 21-29.

Cima F, Ballarin L. 2013. A proposed integrated bioindex for the macrofouling biocoenosis of hard substrata in the lagoon of Venice. Estuarine, Coastal and Shelf Science 130: 190-201.

Clynick, B.G., Chapman, M.G. & Underwood, A.J. 2007. Effects of epibiota on assemblages of fish associated with urban structures. Marine Ecology Progress Series, 332: 201-210.

Costanza R, Darge R, Degroot R, Farber S, Grasso M, Hannon B, Limburg K, Naeem S, Oneill RV, Paruelo J, Raskin RG, Sutton P, Vandenbelt M. 1997. The value of the worlds ecosystem services and natural capital. Nature 387: 253-260.

Cozzoli F, Smolders S, Eelkema M, Ysebaert T, Escaravage V, Temmerman S, Meire P, Herman PMJ, Bouma TJ. 2017. A modeling approach to assess coastal management effects on benthic habitat quality: A case study on coastal defense and navigability. Estuarine, Coastal and Shelf Science 184: 67-82.

Curiel D, Checchin E, Miotti C, Pierini A, Rismondo A. 2014. Praterie a fanerogame marine della laguna di Venezia-aggiornamento cartografico al 2010 e confronto storico. Lav. Society. Venezia. Science. Nature 39: 55-66.

Dafforn KA, Glasby TM, Airoldi L, Rivero NK, Mayer-Pinto M, Johnston EL. 2015. Marine urbanization: an ecological framework for designing multifunctional artificial structures. Frontiers in Ecology and the Environment 13(2): 82-90.

D'Alpaos L. 2010. L'evoluzione morfologica della laguna di Venezia attraverso la lettura di alcune mappe storiche e delle sue mappe idrografiche. Comune di Venezia, Istituzione Centro Previsioni e Segnalazioni Maree Europrint srl, Quinto di Treviso 2010, 110.

Davidson-Arnott R. 2010. Introduction to Coastal Processes and Geomorphology. Cambridge University Press 439.

De Falco G, Tonielli R, Di Martino G, Innangi S, Simeone S, Parnum IM. 2010. Relationships between multibeam backscatter, sediment grain size and Posidonia oceanica seagrass distribution. Continental Shelf Research 30(18): 1941-1950

Defendi V, Kovačević V, Arena F, Zaggia L. 2010. Estimating sediment transport from acoustic measurements in the Venice Lagoon inlets. Continental shelf research 30(8): 883-893.

De Roo S, Troch P. 2015. Evaluation of the Effectiveness of a Living Shoreline in a Confined, Non-Tidal Waterway Subject to Heavy Shipping Traffic. River research and applications 31(8): 1028-1039.

Diesing, M., Green, S.L., Stephens, D., Lark, R.M., Stewart, H.A. and Dove, D., 2014. Mapping seabed sediments: comparison of manual, geostatistical, object-based image analysis and machine learning approaches. Continental Shelf Research, 84: 107-119.

Duck RW, Silva JF. 2012. Coastal lagoons and their evolution: A hydromorphological perspective. Estuarine, Coastal and Shelf Science 110: 2-14.

Durán R, Guillén J, Rivera J, Muñoz A, Lobo FJ, Fernández-Salas LM, Acosta J. 2017. Subaqueous Dunes Over Sand Ridges on the Murcia Outer Shelf. In *Atlas of bedforms in the Western Mediterranean:* 187-192)

Elliott M, Cutts ND. 2004. Marine habitats: loss and gain, mitigation and compensation. Marine Pollution Bulletin 49 (9–10): 671-674.

ESRI, 2016. ArcGis Desktop: Release 10.2. Environmental System Research Institute.

Favero V. 1991. Evoluzione morfologica e trasformazioni ambientali dalla conterminazione lagunare al nostro secolo. In Conterminazione lagunare: storia, ingegneria, politica e diritto nella laguna di Venezia. Proceedings of the Conference Convegno di studio nel bicentenario della conterminazione lagunare; 14-16.

Feldens P, Diesing M, Schwarzer K, Heinrich C, Schlenz B. 2015. Occurrence of flow parallel and flow transverse bedforms in Fehmarn Belt (SW Baltic Sea) related to the local palaeomorphology. Geomorphology 231: 53-62.

Ferrarin C, Tomasin A, Bajo M, Petrizzo A, Umgiesser G. 2015. Tidal changes in a heavily modified coastal wetland. Continental Shelf Research 101: 22-33.

Ferrario F, Iveša L, Jaklin A, Perkol-Finkel S, Airoldi L, 2016. The overlooked role of biotic factors in controlling the ecological performance of artificial marine habitats. Journal of Applied Ecology 53 (1): 16-24.

Finney SC, Edwards LE. 2016. The “Anthropocene” epoch: Scientific decision or political statement. gsa Today 26(3): 3-4.

Flemming BW. 2000. The role of grain size, water depth and flow velocity as scaling factors controlling the size of subaqueous dunes. In *Marine sandwave dynamics, international workshop*; 23-24.

Folk RL, Ward WC. 1957. Brazos River bar: a study in the significance of grain size parameters. Journal of Sedimentary Research 27(1).

Fontolan G, Pillon S, Quadri FD, Bezzi A. 2007. Sediment storage at tidal inlets in northern Adriatic lagoons: Ebb-tidal delta morphodynamics, conservation and sand use strategies. Estuarine, Coastal and Shelf Science 75(1-2): 261-277.

Foody GM. 2002. Status of land cover classification accuracy assessment. Remote sensing of environment 80(1): 185-201.

Fraccascia S, Winter C, Ernstsen VB, Hebbeln D. 2016. Residual currents and bedform migration in a natural tidal inlet (Knudedyb, Danish Wadden Sea). Geomorphology 271: 74-83.

Fredsøe J, Sumer BM. 1997. Scour at the round head of a rubble-mound breakwater. Coast. Eng. 29(3-4), 231-262.

Gačić M, Mosquera IM, Kovačević V, Mazzoldi A, Cardin V, Arena F, Gelsi G. 2004. Temporal variations of water flow between the Venetian lagoon and the open sea. Journal of Marine systems 51(1-4): 33-47.

Gatto P, Carbognin L. 1981. The Lagoon of Venice: natural environmental trend and man-induced modification/La Lagune de Venise: l'évolution naturelle et les modifications humaines. Hydrological Sciences Journal 26(4): 379-391.

Ghezzo M, Guerzoni S, Cucco A, Umgiesser G. 2010. Changes in Venice Lagoon dynamics due to construction of mobile barriers. Coastal Engineering 57(7): 694-708.

Glasby TM, Connell SD, Holloway MG, Hewitt CL, 2007. Nonindigenous biota on artificial structures: Could habitat creation facilitate biological invasions? Marine Biology 151: 887-895.

Gonenc IE, Wolflin JP. 2005, Coastal Lagoons: Ecosystem Processes and Modeling for Sustainable Use and Development 500, CRC Press, Boca Raton, Fla.

Goudie A. 1993. Human influence in geomorphology. In Geomorphology: the Research Frontier and Beyond; 37-59.

Grøsvik BE, Prokhorova T, Eriksen E, Krivosheya P, Horneland PA, Prozorkevich D. 2018. Assessment of Marine Litter in the Barents Sea, a Part of the Joint Norwegian–Russian Ecosystem Survey. Frontiers in Marine Science 5: 72.

Hamilton C. 2016. The Anthropocene as rupture. The Anthropocene Review 3(2): 93-106.

Hasan RC, Ierodiaconou D, Laurenson L, Schimel A, 2014. Integrating multibeam backscatter angular response, mosaic and bathymetry data for benthic habitat mapping. PLOS ONE, 9(5), p.e97339.

Hayes MO, FitzGerald DM. 2013. Origin, evolution, and classification of tidal inlets. Journal of Coastal Research 69(1): 14-33.

Healy T, Mathew J, de Lange W, Black K. 1997. Adjustments toward equilibrium of a large flood-tidal delta after a major dredging program, Tauranga Harbour, New Zealand. Coastal Engineering 1996: 3284-3294.

Hickin EJ. 1974. The development of meanders in natural river-channels. American journal of science 274(4): 414-442.

Hook RL. 1994. On the efficiency of humans as geomorphic agents. A publication of the Geological Society of America 4(9): 222-225.

Ierodiaconou D, Monk J, Rattray A, Laurenson L, Versace VL. 2011. Comparison of automated classification techniques for predicting benthic biological communities using hydroacoustics and video observations. Continental Shelf Research 31(2): S28-S38.

Ierodiaconou D, Schimel A C, Kennedy D, Monk J, Gaylard G, Young M, Diesin M, Rattray A, 2018. Combining pixel and object based image analysis of ultra-high resolution multibeam bathymetry and backscatter for habitat mapping in shallow marine waters. Marine Geophysical Research, pp.1-18.

Jenks GF. 1967. The Data Model Concept in Statistical Mapping, International Yearbook of Cartography 7: 186–190

Jeuken MCJL, Wang ZB. 2010. Impact of dredging and dumping on the stability of ebb–flood channel systems. Coastal Engineering 57(6): 553-566.

Kammann U, Aust MO, Bahl H, Lang T. 2017. Marine litter at the seafloor–Abundance and composition in the North Sea and the Baltic Sea. Marine pollution bulletin 127: 774-780.

Katayama, T., Irie, I., Kawakami, T., 1974. Performance of offshore breakwaters of the Niigata coast. Coastal Engin. Japan, 17, 129-139.

Kerner M. 2007. Effects of deepening the Elbe Estuary on sediment regime and water quality. Estuarine, coastal and shelf science 75(4): 492-500.

Kjerfve B. 1994. Coastal lagoon processes. Elsevier, Amsterdam, The Netherlands. Amsterdam: Elsevier: 9–39

Klaucke I, Hesse R. 1996. Fluvial features in the deep-sea: new insights from the glacigenic submarine drainage system of the Northwest Atlantic Mid-Ocean Channel in the Labrador Sea. *Sedimentary Geology 106*(3-4): 223-234.

Kołodyńska-Gawrysiak R, Poesen J. 2017. Closed depressions in the European loess belt–Natural or anthropogenic origin? Geomorphology: 288: 111-128.

Lamarche G, Lurton X, Verdier AL, Augustin JM. 2011. Quantitative characterisation of seafloor substrate and bedforms using advanced processing of multibeam backscatter—Application to Cook Strait, New Zealand. Continental Shelf Research 31(2): S93-S109.

Lecours V, Devillers R, Simms AE, Lucieer VL, Brown CJ. 2017. Towards a framework for terrain attribute selection in environmental studies. Environmental Modelling & Software 89: 19-30.

1161 Lecours V, Devillers R, Lucieer VL, Brown CJ. 2017. Artefacts in marine digital terrain models: a multiscale analysis of their impact on the derivation of terrain attributes. IEEE Transactions on Geoscience and Remote Sensing 55(9): 5391-5406.

1166 Lillycrop WJ and Hughes SA.1993. Scour hole problems experienced by the Corps of Engineers. Data presentation and summary. Miscellaneous papers. CERC-93-2, US Army Engineer Waterways Experiment Station, Coastal Engineering Research Center, Vicksburg, MS.

1171 Lucieer V, Hill NA, Barrett NS, Nichol S. 2013. Do marine substrates 'look' and 'sound' the same? Supervised classification of multibeam acoustic data using autonomous underwater vehicle images. Estuarine, Coastal and Shelf Science 117: 94-106.

1176 Luisetti T, Turner RK, Jickells T, Andrews J, Elliott M, Schaafsma M, Beaumont N, Malcolm S, Burdon D, Adams C, Watts W. 2014. Coastal Zone Ecosystem Services: from science to values and decision making; a case study. Science of the Total Environment 493: 682-693.

1181 Madricardo F, Donnici S. 2014. Mapping past and recent landscape modifications in the Lagoon of Venice through geophysical surveys and historical maps. Anthropocene 6: 86-96.

Madricardo F, Foglini F, Kruss A, Ferrarin C, Pizzeghello NM, Murri C, Rossi M, Bajo M, Bellafiore D, Campiani E, Fogarin S, Grande V, Janowski L, Keppel E, Leidi E, Lorenzetti G, Maicu F, Maselli V, Mercorella A, Montereale Gavazzi G, Minuzzo T, Pellegrini C, Petrizzo A, Prampolini M, Remia A, Rizzetto F, Rovere M, Sarretta A, Sigovini M, Sinapi L, Umgiesser G, Trincardi F. 2017. High resolution multibeam and hydrodynamic datasets of tidal channels and inlets of the Venice Lagoon. Scientific data 4, 170121.

Madricardo F, Rizzetto F. 2018. Shallow Coastal Landforms. In Submarine Geomorphology: 161-183.

Maes T, Barry J, Leslie HA, Vethaak AD, Nicolaus EEM, Law RJ, Lyons BP, Martinez R, Harley B, Thain JE. 2018. Below the surface: Twenty-five years of seafloor litter monitoring in coastal seas of North West Europe (1992–2017). Science of the Total Environment 630: 790-798.

Magistrato alle Acque di Venezia. 1997. Interventi alle bocche lagunari per la regolazione dei flussi di marea - Studio di impatto ambientale del progetto di massima, Allegato 6, Tema 5, 163.

Magrini G. 1933. La Laguna di Venezia, in La Laguna di Venezia, Monografia coordinata da G. Magrini, Delegazione Italiana della Commissione per l'esplorazione scientific a del Mediterraneo, Atlante II, C. Ferrari, Venezia 1933.

Marriner N, Flaux C, Morhange C, Kaniewski D. 2012. Nile Delta's sinking past: Quantifiable links with Holocene compaction and climate-driven changes in sediment supply? Geology 40(12): 1083-1086.

Mayer L, Jakobsson M, Allen G, Dorschel B, Falconer R, Ferrini V, Lamarche G, Snaith H, Weatherall P. 2018. The Nippon Foundation—GEBCO Seabed 2030 Project: The quest to see the world's oceans completely mapped by 2030. Geosciences 8(2):63.

McGonigle C, Collier JS. 2014. Interlinking backscatter, grain size and benthic community structure. Estuarine, Coastal and Shelf Science 147: 123-136.

Molinaroli E, Guerzoni S, Sarretta A, Cucco A, Umgiesser G. 2007. Links between hydrology and sedimentology in the Lagoon of Venice, Italy. Journal of Marine Systems 68(3-4): 303-317.

Molinaroli E, Guerzoni S, Sarretta A, Masiol M, Pistolato M. 2009. Thirty-year changes (1970 to 2000) in bathymetry and sediment texture recorded in the Lagoon of Venice sub-basins, Italy. Marine Geology 258(1-4): 115-125.

Monge-Ganuzas M, Cearreta A, Evans G. 2013. Morphodynamic consequences of dredging and dumping activities along the lower Oka estuary (Urdaibai Biosphere Reserve, southeastern Bay of Biscay, Spain). Ocean & coastal management 77: 40-49.

Montereale Gavazzi G, Madricardo F, Janowski L, Kruss A, Blondel P, Sigovini M, Foglini F. 2016. Evaluation of seabed mapping methods for fine-scale classification of extremely shallow benthic habitats–application to the Venice Lagoon, Italy. Estuarine, Coastal and Shelf Science 170: 45-60.

Montereale-Gavazzi, G., Roche, M., Lurton, X., Degrendele, K., Terseleer, N. and Van Lancker, V., 2018. Seafloor change detection using multibeam echosounder backscatter: Case study on the Belgian part of the North Sea. Marine Geophysical Research, 39(1-2), pp.229-247.

Newell R., Seiderer LJ, Hitchcock DR. 1998. The impact of dredging works in coastal waters: a review of the sensitivity to disturbance and subsequent recovery of biological resources on the sea bed. Oceanography and Marine Biology: An Annual Review 36: 127-178.

Noormets R, Ernstsen VB, Bartholomä A, Flemming BW, Hebbeln D, 2006. Implications of bedform dimensions for the prediction of local scour in tidal inlets: a case study from the southern North Sea. Geo-Marine Letters, 26(3):165-176.

Oost AP, Hoekstra P, Wiersma A, Flemming B, Lammerts EJ, Pejrup M, Hofstede J, Van der Valk B, Kiden P, Bartholdy J, Van der Berg MW, Vos PC, de Vries S, Wang ZB. 2012. Barrier island management: Lessons from the past and directions for the future. Ocean & coastal management 68: 18-38.

Ouillon S. 2018. Why and How Do We Study Sediment Transport? Focus on Coastal Zones and Ongoing Methods. Water 10(4):390.

Paulo D, Manent P, Barrio JM, Alvares Serrao E, Alberto F. 2016. Recruit survival of Cymodocea nodosa along a depth gradient. CAHIERS DE BIOLOGIE MARINE 57(2): 137-144.

Perkins MJ, Ng TP, Dudgeon D, Bonebrake TC, Leung K M. 2015. Conserving intertidal habitats: what is the potential of ecological engineering to mitigate impacts of coastal structures? Estuarine, Coastal and Shelf Science 167: 504-515.

Pham CK, Ramirez-Llodra E, Alt CH, Amaro T, Bergmann M, Canals M, Company JB, Davies J, Duineveld G, Galgani F, Howell KL, Huvenne VA, Isidro E, Jones DOB, Lastras G, Morato T, Gomes-Pereira JN, Purser A, Stewart H, Tojeira I, Tubau X, Van Rooij D, Tyler PA. (2014). Marine litter distribution and density in European seas, from the shelves to deep basins. PloS one 9(4), e95839.

Pister B. 2009. Urban marine ecology in southern California: the ability of riprap structures to serve as rocky intertidal habitat. Marine Biology 156(5): 861-873.

Poesen J. 2018. Soil erosion in the Anthropocene: Research needs. Earth Surface Processes and Landforms 43(1): 64-84.

Rapaglia J, Zaggia L, Ricklefs K, Gelinas M, Bokuniewicz H. 2011. Characteristics of ships' depression waves and associated sediment resuspension in Venice Lagoon, Italy. Journal of Marine Systems 85(1-2): 45-56.

Rattray A, Ierodiaconou D, Monk J, Versace V L and Laurenson L J B, 2013. Detecting patterns of change in benthic habitats by acoustic remote sensing. Marine Ecology-Progress Series, 477:1-13.

Reddy NA, Vikas M, Rao S, Seelam JK. 2015. Classification of tidal inlets along the central east coast of India. Procedia Engineering 116: 922-931.

Reggiannini M, Salvetti O. 2017. Seafloor analysis and understanding for underwater archeology. Journal of Cultural Heritage 24: 147-156.

Renaud, F.G., Syvitski, J.P., Sebesvari, Z., Werners, S.E., Kremer, H., Kuenzer, C., Ramesh, R., Jeuken, A. and Friedrich, J., 2013. Tipping from the Holocene to the Anthropocene: How threatened are major world deltas?. *Current Opinion in Environmental Sustainability*, *5*(6): 644-654.

Rodrigues V, Estrany J, Ranzini M, de Cicco V, Martín-Benito JMT, Hedo J, Lucas-Borja ME. 2017. Effects of land use and seasonality on stream water quality in a small tropical catchment: The headwater of Córrego Água Limpa, São Paulo (Brazil). *Science of The Total Environment*: 1553-1561.

Sarretta A, Pillon S, Molinaroli E, Guerzoni S, Fontolan G. 2010. Sediment budget in the Lagoon of Venice, Italy. Continental Shelf Research 30(8): 934-949.

Sato, S., Tanaka, N., and Irie, I. 1968. Study on scouring at the foot of coastal structures. Proceedings of 11th Coastal Engineering Conference, American Society of Civil Engineers, 579-598.

Small C, Nicholls RJ. 2003. A global analysis of human settlement in coastal zones. Journal of coastal research: 584-599.

Stanic S, Briggs KB, Fleischer P, Ray RI, Sawyer WB. 1988. Shallow-water high-frequency bottom scattering off Panama City, Florida. The Journal of the Acoustical Society of America 83(6): 2134-2144.

Story M, Congalton RG. 1986. Accuracy Assessment: A User's Perspective. Photogrammetric Engineering and Remote Sensing 52: 397-399.

Sumer, B.M., Fredsøe, J., 1997. Scour at the head of a vertical-wall breakwater. Coast. Eng. 29(3-4), 201-230.

Sumer, B.M., Whitehouse, R.J.S., Tørum, A., 2001. Scour around coastal structures: a summary of recent research. Coast Eng. 44(2), 153– 190.

Svane I., Petersen JK, 2001. On the Problems of Epibioses, Foulingand Artificial Reefs, a Review. Marine Ecology, 22 (3): 169-188.

Syvitski JP, Vörösmarty CJ, Kettner AJ, Green P. 2005. Impact of humans on the flux of terrestrial sediment to the global coastal ocean. Science 308(5720): 376-380.

Tagliapietra D, Sigovini M, Magni P. 2012. Saprobity: a unified view of benthic succession models for coastal lagoons. Hydrobiologia, 686: 15-28.

Tambroni N, Seminara G. 2006. Are inlets responsible for the morphological degradation of Venice Lagoon. Journal of Geophysical Research: Earth Surface 111.

Tarolli P. 2014. High-resolution topography for understanding Earth surface processes: Opportunities and challenges. Geomorphology 216: 295-312.

Teatini P, Isotton G, Nardean S, Ferronato M, Mazzia A, Da Lio C, Zaggia L, Bellafiore D, Zecchin M, Baradello L, Cellone F, Corami F, Gambaro A, Libralato G, Morabito E, Volpi Ghirardini A, Broglia R, Zaghi S, Tosi L. 2017. Hydrogeological effects of dredging navigable canals through lagoon shallows. A case study in Venice. Hydrology and Earth System Sciences 21(11), 5627.

Temmerman S, Meire P, Bouma TJ, Herman PM, Ysebaert T, De Vriend HJ (2013). Ecosystem-based coastal defence in the face of global change. Nature 504(7478): 79.

Tosi L, Teatini P, Strozzi T. 2013. Natural versus anthropogenic subsidence of Venice. Scientific reports, 3, 2710.

Trincardi F, Barbanti A, Bastianini M, Benetazzo A, Cavaleri L, Chiggiato J, Papa A, Pomaro A, Sclavo M, Tosi L, Umgiesser G. 2016. The 1966 flooding of Venice: what time taught us for the future. Oceanography 29(4): 178-186.

1358 Turner MG, 1989. Landscape ecology - the effect of pattern on process. Annual Review of Ecology and Systematics 20: 171-197.

1361 Valdenegro-Toro M. 2016. Submerged marine debris detection with autonomous underwater vehicles. In Robotics and Automation for Humanitarian Applications (RAHA), 2016 International Conference 1-7.

1365 Van Maren DS, Van Kessel T, Cronin K, Sittoni L. 2015. The impact of channel deepening and dredging on estuarine sediment concentration. *Continental Shelf Research 95*: 1-14.

1369 Van Raalte GH. 2006. Dredging techniques: adaptations to reduce environmental impact. Dredging in Coastal Waters. Taylor and Francis, London, 1-40.

1372 Vatova A., 1940. Le zoocenosi della Laguna veneta. Thalassia, 3(10): 1-28.

1374 Vatova A., 1949. La fauna bentonica dell'Alto e medio Adriatico. Nova Thalassia I. (3): pp. 110.

1377 Villatoro MM, Amos CL, Umgiesser G, Ferrarin C, Zaggia L, Thompson CE, Are D. 2010. Sand transport measurements in Chioggia inlet, Venice lagoon: Theory versus observations. Continental Shelf Research 30(8): 1000-1018.

1381 Wang ZY, Li Y, He Y. 2007. Sediment budget of the Yangtze River. Water Resources Research, 43(4).

1384 Wanless HR. 1981. Barrier Islands from the Gulf of St. Lawrence to the Gulf of Mexico. Sedimentary Geology 30: 153-154.

1387 Wasson K, Fenn K, Pearse JS, 2005. Habitat differences in marine invasions of central California. Biological Invasions (2005) 7: 935–948.

1390 Williams, C.B. 1964. Patterns in the Balance of Nature. Academic Press, London.

1392 Williams SJ. 2013. Sea-level rise implications for coastal regions. Journal of Coastal Research 63(1): 184-196.

1395 Winterwerp JC, Wang ZB, van Braeckel A, van Holland G, Kösters F. 2013. Man-induced regime shifts in small estuaries—II: a comparison of rivers. Ocean Dynamics 63(11-12): 1293-1306.

1399 Wright D, Lundblad E, Larkin E, Rinehart R, Murphy J, Cary-Kothera L, Draganov K. 2005. ArcGIS Benthic Terrain Modeler (BTM), v. 3.0. Environmental Systems Research Institute, NOAA Coastal Services Center, Massachusetts Office of Coastal Zone Management.

Yu J, Henrys SA, Brown C, Marsh I, Duffy G. 2015. A combined boundary integral and Lambert's Law method for modelling multibeam backscatter data from the seafloor. Continental Shelf Research 103: 60-69.

Zaggia L, Lorenzetti G, Manfé G, Scarpa GM, Molinaroli E, Parnell KE, Rapaglia P, Gionta M, Soomere T. 2017. Fast shoreline erosion induced by ship wakes in a coastal lagoon: Field evidence and remote sensing analysis. PloS one 12(10): e0187210.

Zecchin M, Baradello L, Brancolini G, Donda F, Rizzetto F, Tosi L. 2008. Sequence stratigraphy based on high-resolution seismic profiles in the late Pleistocene and Holocene deposits of the Venice area. Marine Geology 253(3-4): 185-198.

Zhu G, Xie Z, Xu X, Ma Z, Wu Y. 2016. The landscape change and theory of orderly reclamation sea based on coastal management in rapid industrialization area in Bohai Bay, China. Ocean and Coastal Management (133): 128-137.

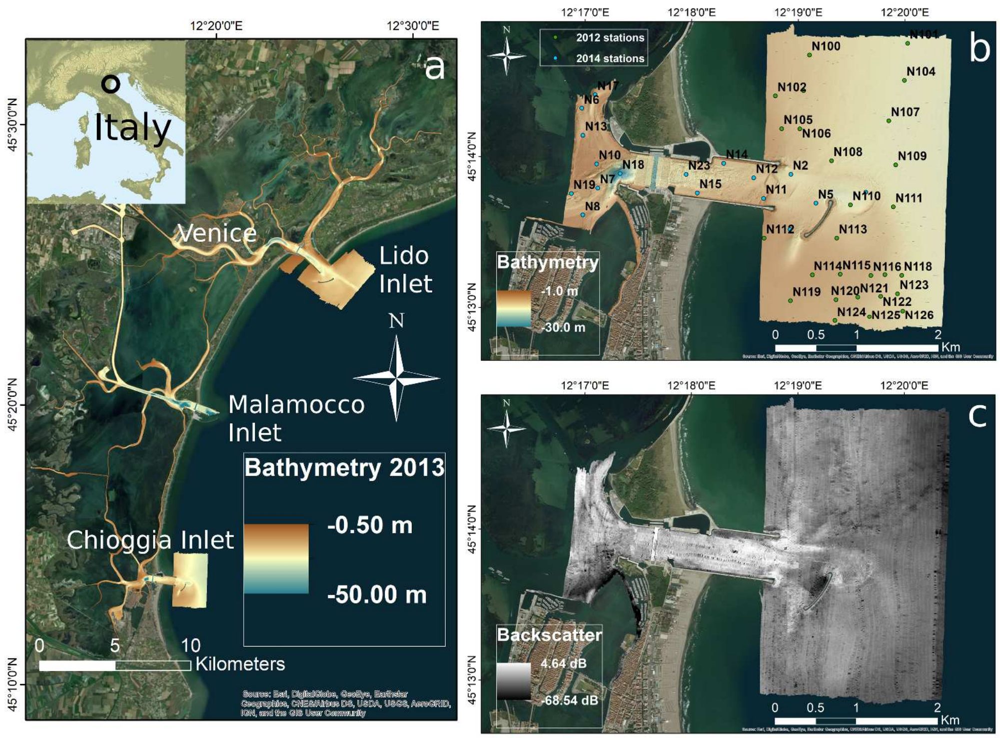

Fig 1. a) The bathymetry of the tidal channels and inlets of the Venice Lagoon collected during the CNR ISMAR survey in 2013 (Madricardo et al., 2017); b) the bathymetry of the Chioggia inlet with the location of the sampling stations for 2012 (green) and 2014 (light blue); c) the backscatter mosaic extracted from the multibeam data.

347x258mm (300 x 300 DPI)

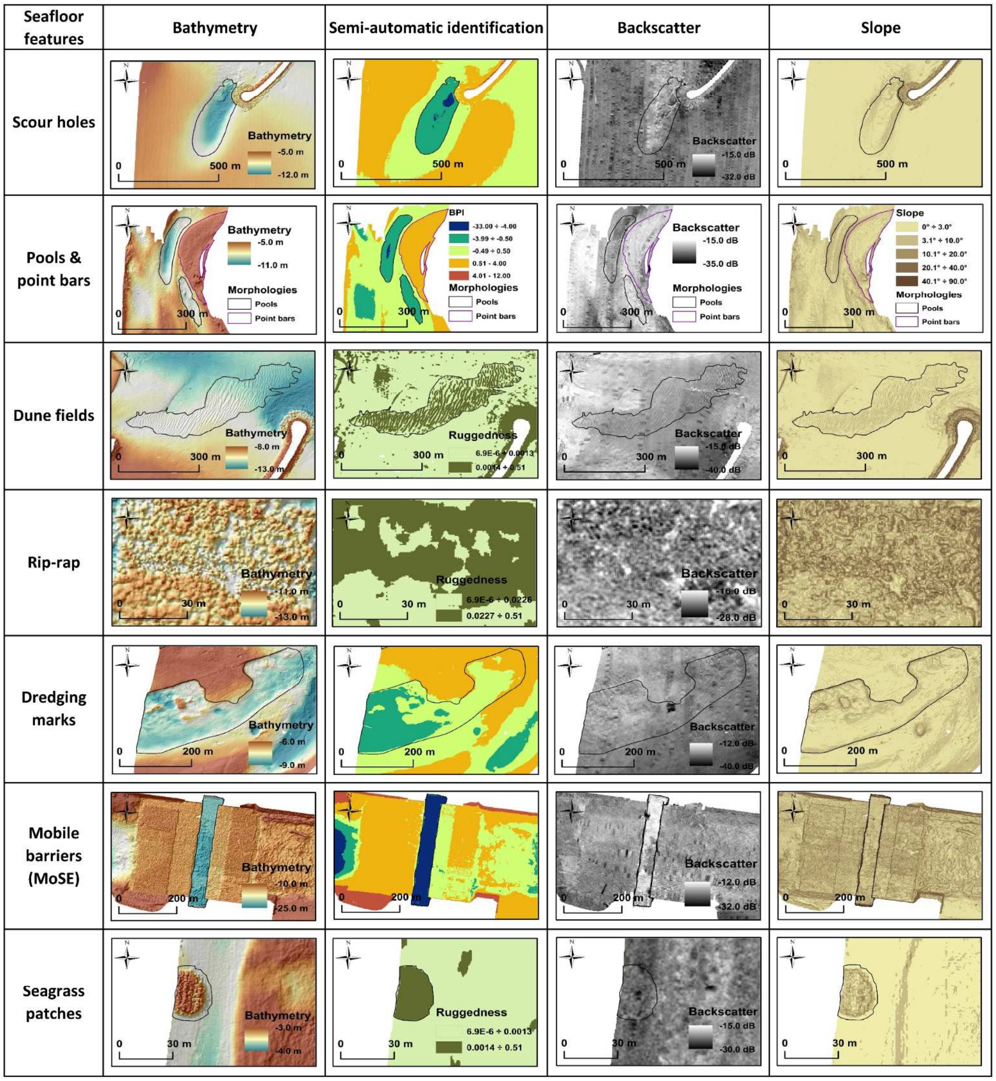

Fig. 2. Cllassified morphologies with their bathymetry (first column with 5 times vert. exaggeration), with the terrain attribute used for the semi-automatic identification (second column); their backscatter mosaics (third column) and their slope (fourth column).

265x288mm (300 x 300 DPI)

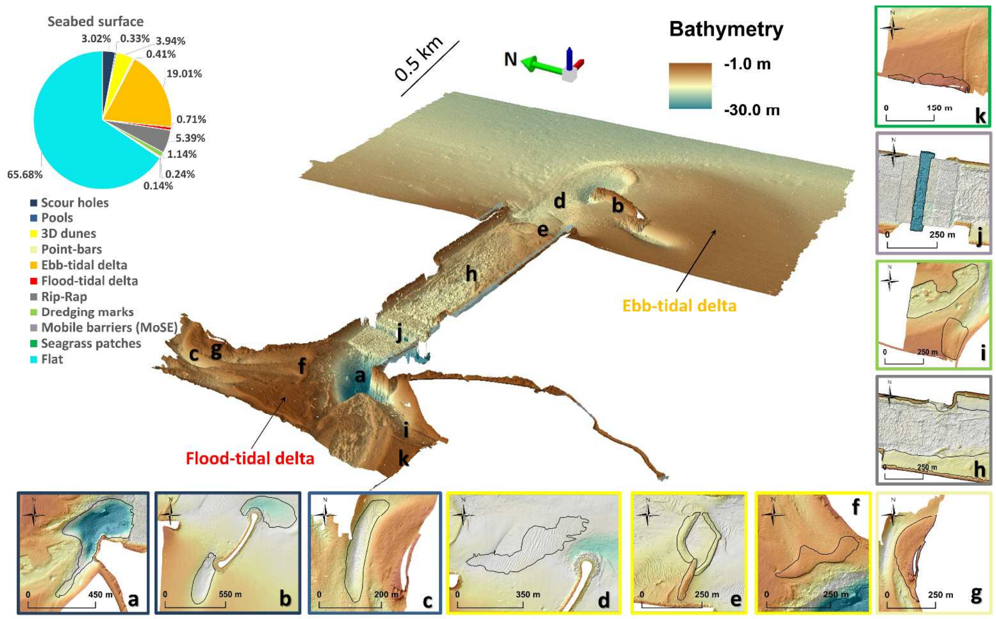

Fig. 3. 3D representation of the Chioggia Inlet morphology with the identified seafloor features: a) and b) scour holes at hard structures; c) tidal channel pool; d) dune field; e) and f) large dunes; g) tidal channel point bar; h) rip-rap; i) dredging marks; j) MoSE trench; k) sea-grass patches; The pie chart in the upper left corner represents the percentage areas occupied by each feature class with respect of the total surveyed area.

595x364mm (300 x 300 DPI)

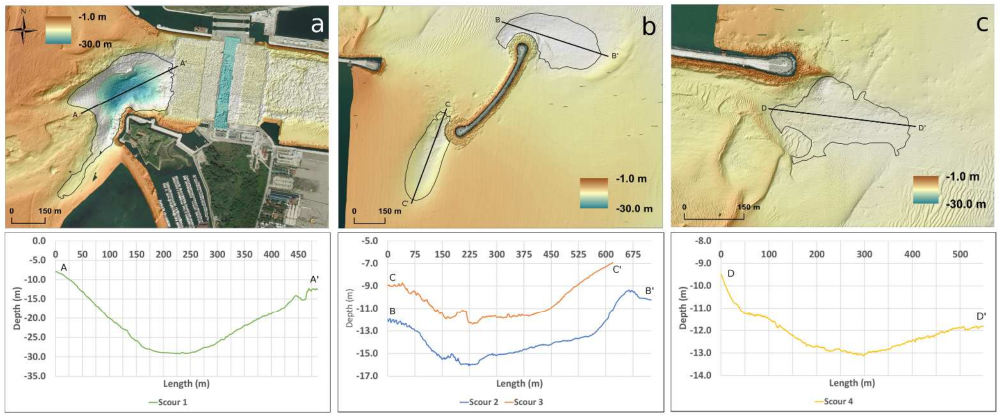

Fig.4. Scour holes and their profiles: a) the deepest scour hole on lagoon side; b) the scour holes at breakwater tips c) the smallest scour hole near the northern jetty.

421x175mm (300 x 300 DPI)

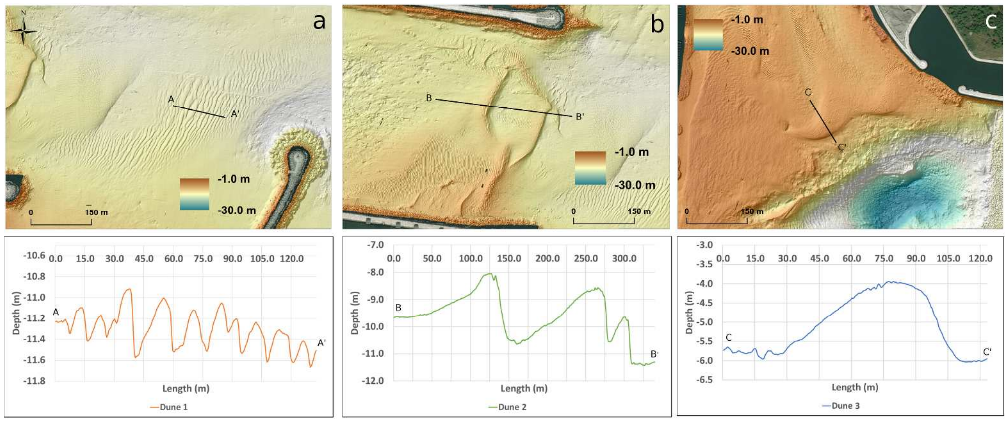

Fig.5. Dune fields and their profiles: a) dune field on the seaside; b) large dunes near the eastern inlet entrance (seaside); c) large dunes near the western inlet entrance (lagoon side).

431x179mm (300 x 300 DPI)

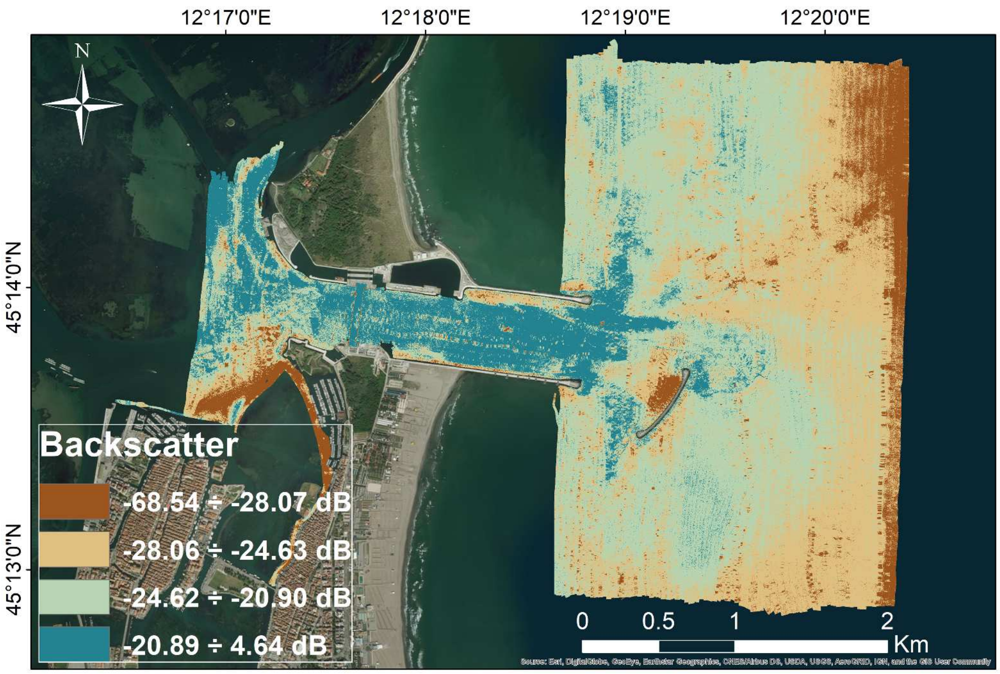

Fig. 6. Backscatter Classified with the Jenks' algorithm in four sediment classes: Slightly Gravelly Muddy Sand_Muddy Sand_Slightly Gravelly Sandy Mud SGMS_MS_SGSM (brown), Sand S (beige), Slightly Gravelly Sand SGS (light green), Sandy Gravel_Gravelly Sand SG_GS (dark green), corresponding to very low backscatter intensity: < - 28.07 dB; medium-low backscatter intensity: -28.07 ÷ -24.63 dB; medium-high backscatter intensity: -24.63 ÷ -20.90 dB; very high backscatter intensity: > -20.90 dB, respectively.

373x252mm (300 x 300 DPI)

Class	BS range (dB)	Original BS	Classified BS	Drop-frame	Description
1 - Coarse shell detritus	> -20.90		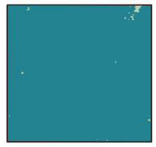		Seafloor completely covered by coarse shell detritus, D50 typical of gravels, poor sorting, scarse vegetation cover. Observed biota includes both infauna and encrusting epifauna (such as Serpulidae and Actiniaria). Occasionally dense Ophiothrix beds are observed.
2 - Sand with sparse shell detritus	-24.63 ÷ -20.90	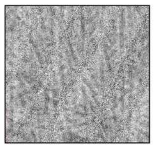	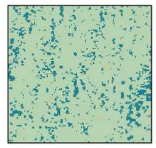	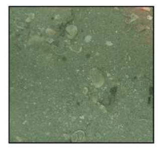	Coarse sand seafloors with sparse shell detritus and moderate sorting, vegetation absent. Infauna and vagile epifauna (such as *Carcinus aestuarii* and *Nassarius nitidus*) prevail.
3 - Bare sand	-28.07 ÷ -24.63	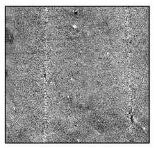	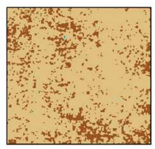	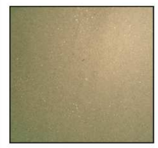	Well sorted sand seafloors, absence of coarse fragments and vegetation, D50 typical of medium sands. Epifauna rarely observed.
4 - Lagoon mudflat	< -28.07				Very well sorted fine muddy, poor presence of shells. Typical mudflat sediment. Significant vegetation cover (mainly *Ulva* sp.). Observed taxa include vagile epifauna (e.g. *Carcinus aestuarii* and *Nassarius nitidus*).
5 - Muddy sediment	< -28.07		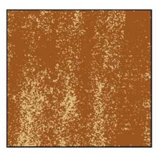		Very well sorted fine sediment, absence of coarse fragments. Significant vegetation cover (mainly *Ulva* sp.). Observed taxa include both infauna (e.g. *Echinocardium cordatum* and Veneridae) and vagile epifauna (e.g. *Carcinus aestuarii*).
6 - Artificial rock bed	Variable	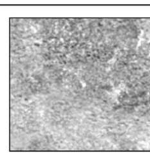	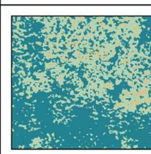		Riprap seafloor characterized by rocky substrata with small mud patches. Presence of macroalgae, encrusting and vagile epifauna (e.g. *Pachygrapsus marmoratus*). Occasionally dense Ophiothrix beds are observed.
7- Seagrass meadow	Variable	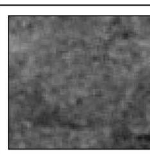	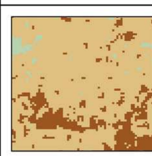		Well sorted fine sediment covered by seagrass *(Cymodocea nodosa)*. Diverse infauna and epifauna assemblages.

Fig. 7. Schematic description of the habitat classes with their backscatter signal, classified backscatter and corresponding seafloor image.

159x210mm (300 x 300 DPI)

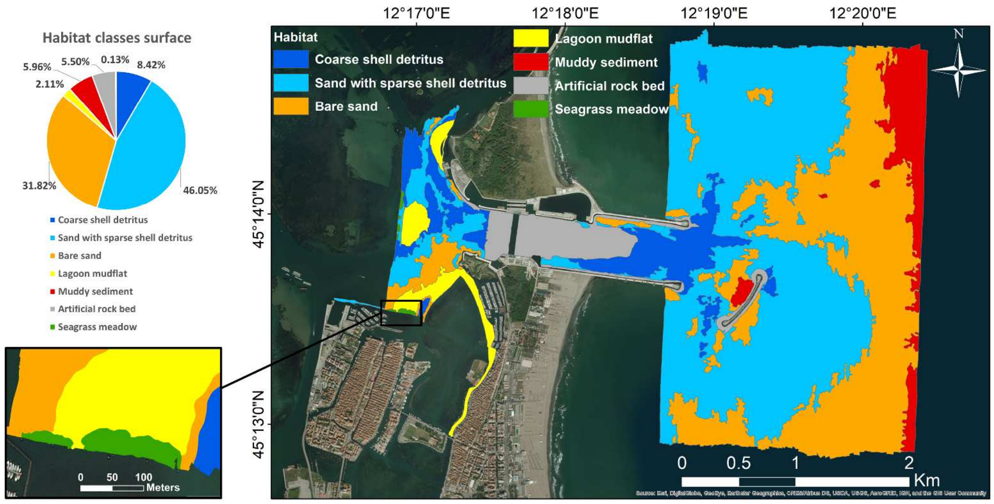

Fig.8. Benthic habitats in the Chioggia Inlet, where the dark blue class represents Coarse Shell Detritus, the light blue Sand with spares shell detritus, the yellow Bare Sand, the red Muddy Sediment, the grey Artificial rock bed and the green the Seagrass meadow. The pie chart shows the relative surface occupied by each benthic habitat class with respect to the total study area.

400x203mm (300 x 300 DPI)

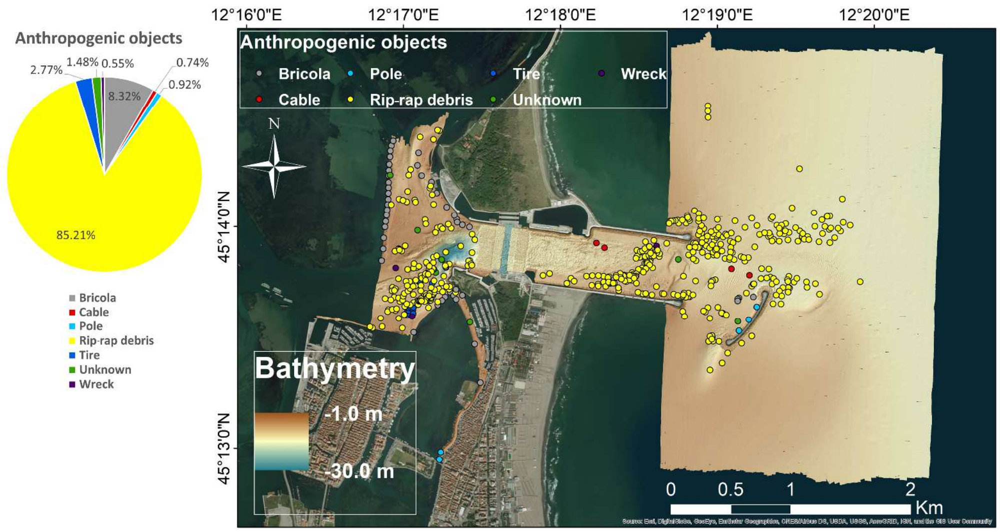

Fig. 9. Anthropogenic objects identified in the study area; The pie chart in the upper right corner represents the percentage number of each object type with respect to the total number of mapped objects.

434x229mm (300 x 300 DPI)

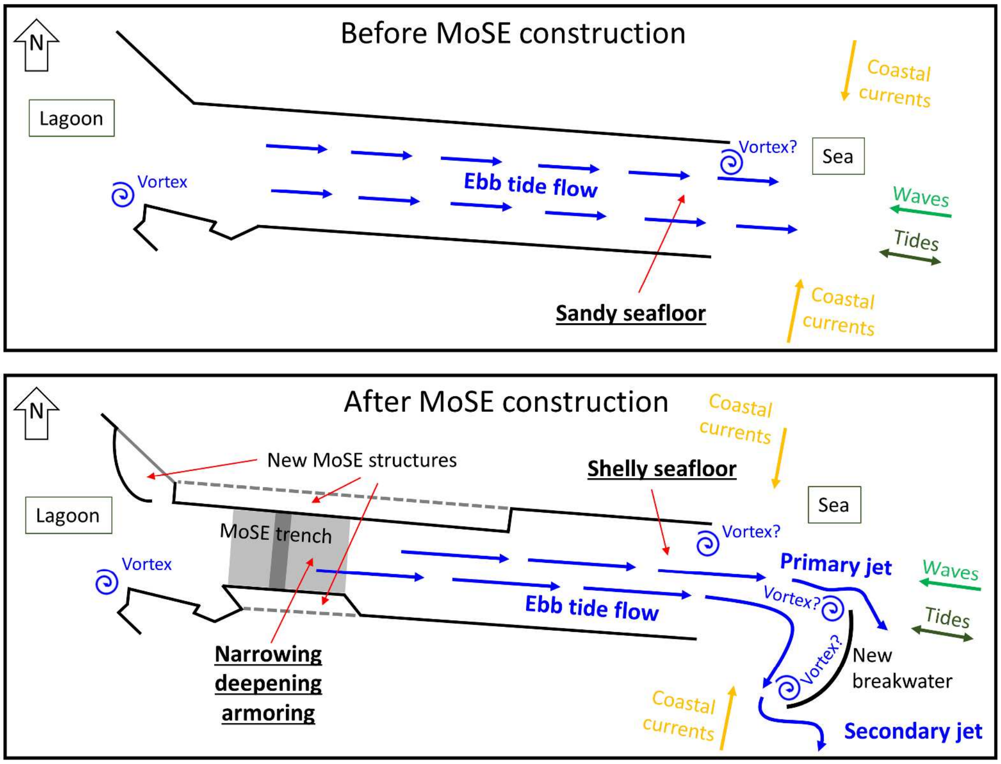

Fig.10. Schematic summary of the dominant processes in the Chioggia inlet before (top) and after (down) the construction of the MoSE hard structures.

258x197mm (300 x 300 DPI)

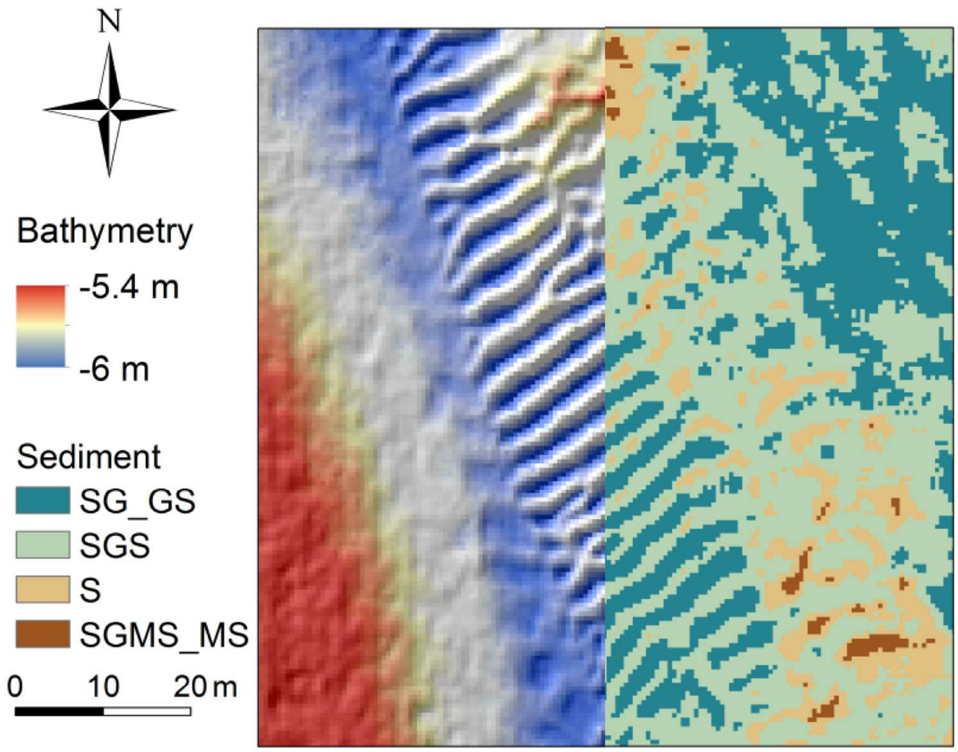

Fig.11. Bathymetry and sediment distribution of a dune field in the Chioggia inlet with sandy gravel_gravelly sand in the troughs (SG_GS) and slightly gravelly sand (SGS) over the crests.

174x136mm (300 x 300 DPI)

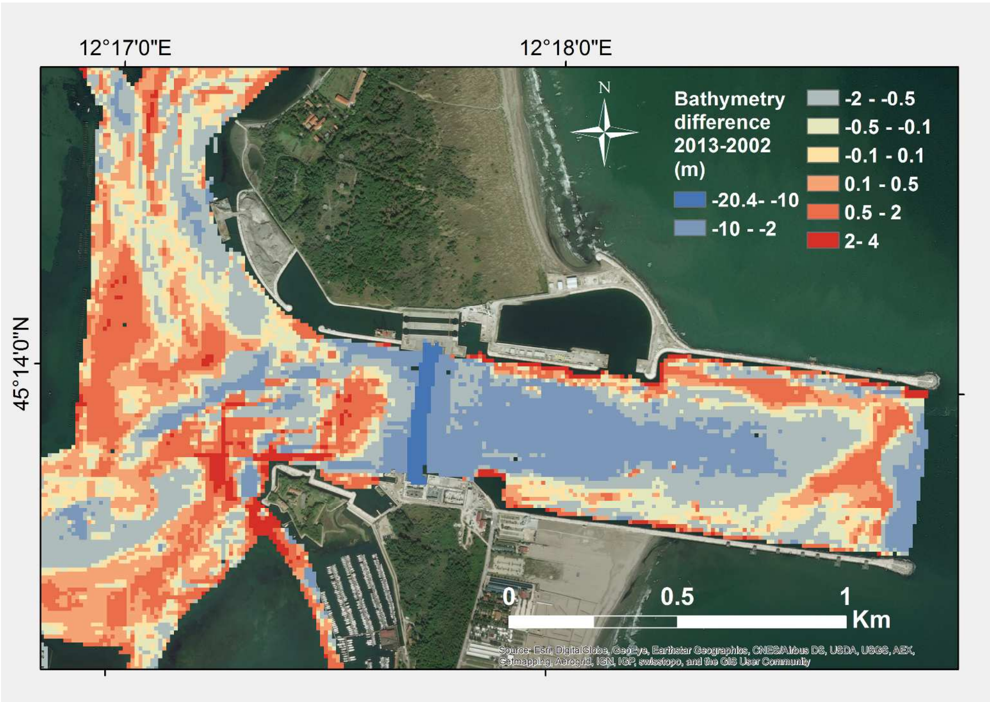

Fig.12. Bathymetric difference between the 2013 and 2002 datasets.

297x209mm (300 x 300 DPI)

Confusion matrix Chioggia 2013

JENKS' classification

		Ground-truth samples			
		SG_GS	*SGS*	*S*	*SGSMS_MS_SGSM*
Classified samples	*SG_GS*	**5**	0	0	1
	SGS	0	**22**	0	1
	S	0	5	**2**	4
	SGSMS_MS_SGSM	0	0	0	**4**
Total ground-truth samples		5	27	2	10
Overall Accuracy (%) = 75					

Total classified	Producer accuracy	User accuracy
6	100	83
23	81	96
11	100	18
4	40	100
44		

Stations	Ripples	Matrix dimension	Sorting	General description
N02	NA	NA	NA	Coarse shell fragments
N03	NA	<_1_mm	WS	Medium sand
N04	NA	<_1_mm	MS	Medium sand
N05	NA	<<_1_mm	WS	Fine sand
N06	NA	NA	NA	Coarse shell fragments
N07	12-20 cm	<_1_mm	WS	Medium sand
N08	NA	<<_1_mm	WS	Fine sand / silt
N10	NA	<_1_mm	PS	Coarse sand + coarse shell fragments
N11	12-40 cm	1_mm	PS	Coarse sand
N12	NA	<_1_mm	WS	Medium sand + coarse shell fragments
N13	20-30 cm	<_1_mm	MS	Medium sand + coarse shell fragments
N14	NA	<<_1_mm	WS	Fine sand
N15	20-30 cm	<_1_mm	WS	Medium sand
N17	6-10 cm	1_mm	MS	Medium sand
N18	NA	<_1_mm	WS	Medium sand + gravel
N19	NA	<<_1_mm	WS	Partially consolidated fine sand / silt

N23	NA	<<_1_mm	WS	Partially consolidated fine sand / silt + rocks
N24	NA	<_1_mm	WS	Medium sand
N25	NA	<<_1_mm	WS	Fine sand / silt

NA = not available NA = not available NA = not available

PS = poor sorted

MS = moderatly sorted

WS = well sorted

Thanatocoenosis	Living biota	Shells coverage %
Abra sp., *Acanthocardia tuberculata, Cerithium* sp., *Chamelea gallina, Mytilus galloprovincialis, Nassarius nitidus,* Ostreidae indet., Pectinidae sp., *Scapharca* sp., Serpulidae indet., *Spisula subtruncata, Tellina* sp., Veneridae indet., *Venerupis aurea*		95
		2
Bittium sp., *Chamelea gallina, Spisula* sp., *Nassarius nitidus,* Solenoidea indet., Veneridae indet.	Actiniaria indet.	4
		0
Cardiidae indet., *Cerithium* sp., *Gibbula* sp., Mytilidae indet., *Nassarius nitidus,* Ostreidae indet., Pectinidae sp., *Ruditapes* sp., *Scapharca* sp., Serpulidae indet., Veneridae indet., *Venerupis aurea*	Actiniaria indet., Pectinidae sp.	100
	Nassarius nitidus	1
	Nassarius indet.	0
Chamelea gallina, Cyclope neritea, Ruditapes sp., Serpulidae indet., *Venerupis aurea*	Bivalvia indet. (siphons)	95
Abra sp., *Bittium* sp., *Loripes lacteus, Mytilus galloprovincialis,* Scaphopoda indet., Serpulidae indet., *Spisula subtruncata, Tellina* sp., Veneridae indet.		65
Acanthocardia tuberculata, Calliostoma sp., *Chamelea gallina, Cyclope neritea, Loripes lacteus,* Mytilidae indet., Pectinidae sp., Serpulidae indet., *Spisula* sp., *Tellina* sp., Veneridae indet., *Venerupis aurea*	Paguroidea indet.	20
Bittium sp., *Chamelea gallina, Glycymeris violacescens, Mytilus galloprovincialis, Scapharca* sp., Scaphopoda indet., Serpulidae indet., Solenoidea indet., Veneridae indet., *Venerupis aurea*		18
	Carcinus aestuarii, Nassarius nitidus	1
Mytilidae indet., Solenoidea indet., Veneridae indet.		2
Bittium sp., Veneridae indet.	*Asterina gibbosa* , *Carcinus aestuarii,* Paguroidea indet.	1
Serpulidae indet., Veneridae indet.	Actiniaria indet., *Ophiothrix* sp.	7
Veneridae indet.		1

Ostreidae indet., Serpulidae indet.	Pachygrapsus marmoratus, *Ophiothrix* sp.	0
Veneridae indet.	*Carcinus aestuarii, Nassarius nitidus*, Paguroidea indet., Tunicata indet. (col.)	1
Veneridae indet.		1

M

Shells density	Average shells size	Macrophytobenthos typology	Macrophytobenthos coverage	Notes
Very high	2 cm	Seagrass fragments		
Very low	0.5 cm			
Very low	1.5 cm	Seagrass fragments		
Very low	NA	Seagrass fragments		
Very high	2.5 cm	Seagrass patch-type 1	5	
Very low	0.5 cm	Seagrass fragments		
Very low	NA			
Very high	1.5 cm			near to Ostreidae indet. thanatocoenosis
Medium	0.5 cm			
Low	1.5 cm			
Low	1.5 cm			
Very low	1 cm	Seagrass fragments		*Ophiothrix* sp. observed nearby
Very low	1 cm			
Very low	0.5 cm	Seagrass fragments		
Very low	0.5 cm	Seagrass fragments		*Ophiothrix* sp. bed (50% coverage)
Very low	0.5 cm	Seagrass fragments		

Very low	NA	Seagrass fragments		Rocks, presence of *Ophiothrix* sp.
Very low	0.5 cm	Seagrass patch-type 2	48	
Very low	1 cm	Seagrass patch-type 3	60	

Very low = < 10%
Low = 10% ÷ 50%
Medium = 50% ÷ 75%
High = 75% ÷ 90%
Very high = > 90%

Type 1 = < 5%
Type 2 = 5% ÷ 50%
Type 3 = 50% ÷ 75%
Type 4 = > 75%

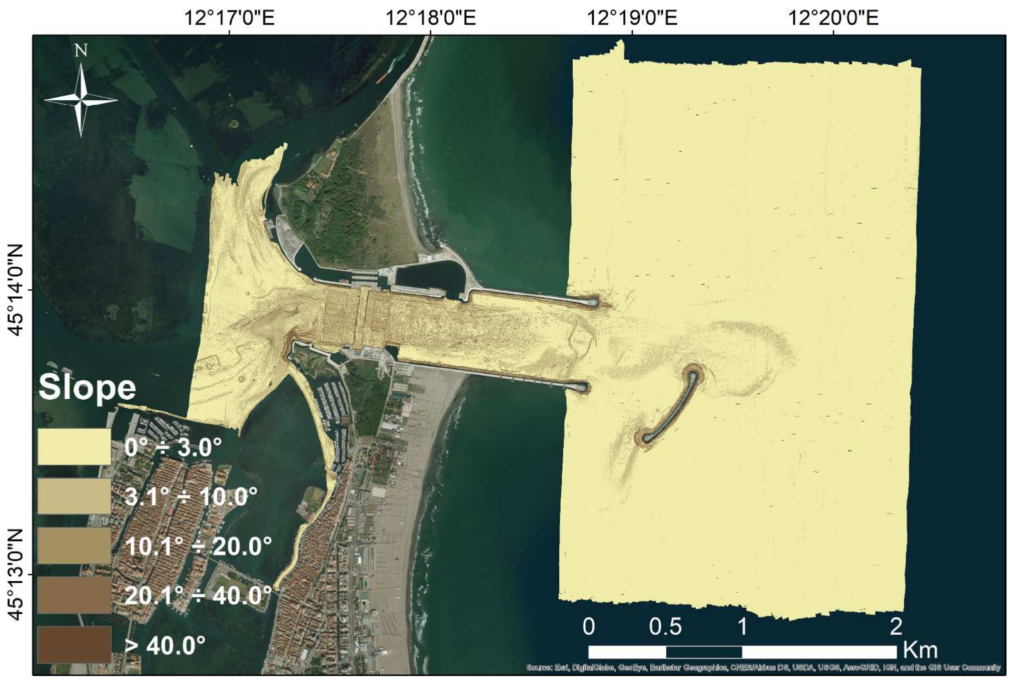

369x246mm (300 x 300 DPI)

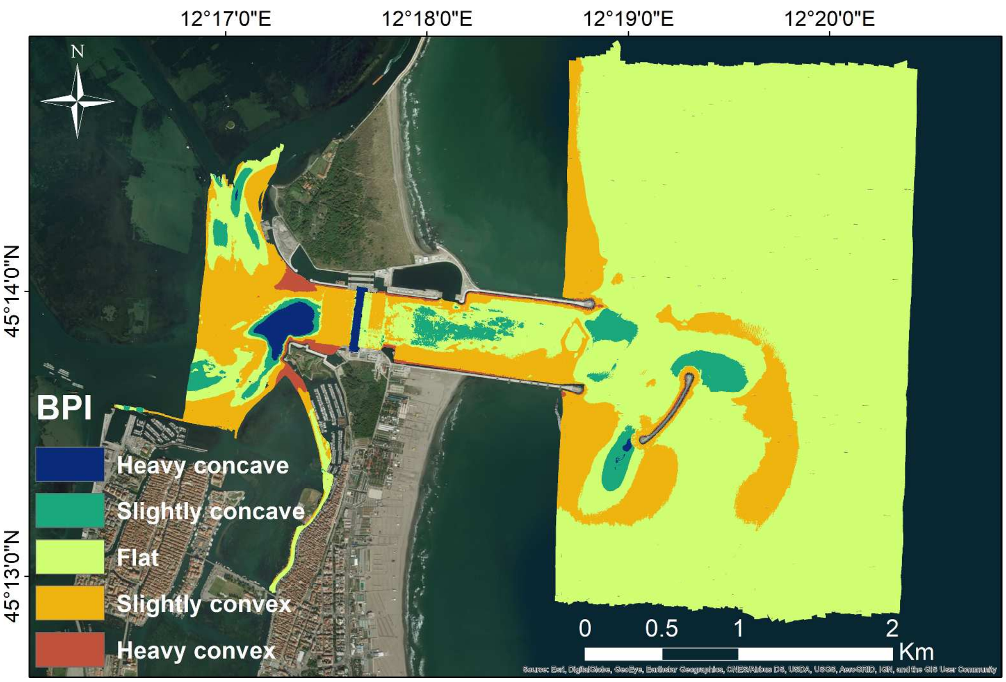

369x246mm (300 x 300 DPI)

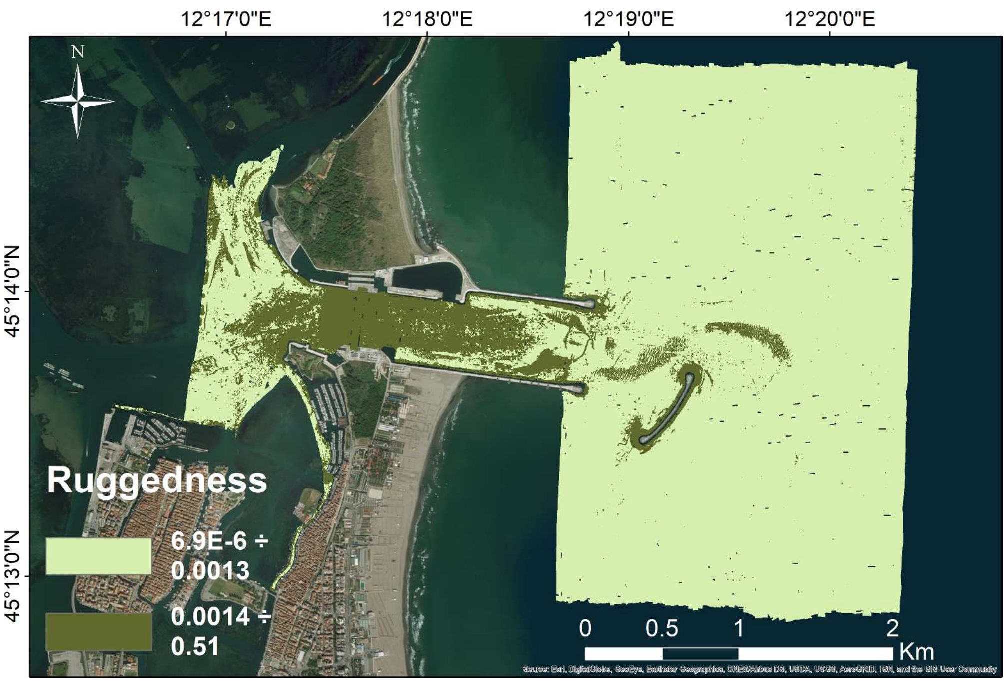

369x246mm (300 x 300 DPI)